ASSESSING RADTRIAGE COLORIMETRIC DOSIMETER RESPONSE TO LOW-DOSE GAMMA-RAY EXPOSURE

A Thesis
submitted to the Faculty of the
Graduate School of Arts and Sciences
of Georgetown University
in partial fulfillment of the requirements for the
degree of
Master of Science
in Health Physics

By

Lindsay Elizabeth Rand, B.A.

Washington, DC
March 29, 2019

ASSESSING RADTRIAGE COLORIMETRIC DOSIMETER RESPONSE TO LOW-DOSE GAMMA-RAY EXPOSURE

Lindsay Elizabeth Rand, B.A.

Thesis Advisor: Luis A. Benevides, Ph.D.

ABSTRACT

There is a need for instantly indicating, easy-to-read, and relatively inexpensive ionizing radiation casualty dosimeters for first responders and members of the general public. One such dosimeter is the RadTriage™ colorimetric dosimeter. Although colorimetric dosimetry has been studied over the past few decades, and widely applied in the medical field, there is a lack of research into understanding how well RadTriage colorimetric dosimeter cards quantify low doses of ionizing radiation (< 50 mSv). Furthermore, research on RadTriage card application to be read post-exposure, including methods to quantify post-exposure readings and fit post-exposure readings with a dose response function, is limited. In this research we use digital scanning methods to read the RadTriage colorimetric dosimeter cards. Digital scanning processes for reading colorimetric dosimeters have previously been studied and applied for use in the medical field and were standardized by the AAPM Report 63 recommendations. The tests performed in this research were used to verify the responsiveness of RadTriage cards across the manufacturer's specified range, 50 mSv to 4000 mSv. Tests were also performed at incremental doses below the manufacture's specified range to determine if application of the digital scanning densitometry method allows for a more systematic, quantitative readout with a greater dynamic range. Finally, tests were conducted with different gamma energies, using Cs-137 (662 keV) and Co-60 (1.17 and 1.33 MeV), and

different dose rates to determine the impact of changes in these variables on the card's response to a given exposure.

We found an exponential dose response function to fit our RadTriage data with a chi-square value of 1.38 and a corresponding probability of fit value of $P = 0.998$. Our exponential fit shows a proportional, linear response at low doses that eventually plateaus at higher doses; this is consistent with the chemical basis of radiochromic dosimeters and with the results of prior research. In analyzing our results, we also found that the RadTriage cards responded with increased sensitivity, marked by a statistically significant differences, at lower dose rates and lower gamma energies. These results suggest that changes in certain exposure characteristics can impact the RadTriage dose response. The RadTriage dose response was also compared to the thermoluminescent detector response; in comparison, the thermoluminescent detectors had less response variation under different exposure characteristics. The results from this comparison suggest that both types of dosimeters, thermoluminescent and colorimetric, had strengths and weaknesses. RadTriage cards are able to be handed off rapidly without pre-testing, they allow for real-time indication of doses above a threshold, they are inexpensive, and they can be read visually and by commercially available digital scanners. However, our research shows that certain dose characteristics such as dose rate and photon energy impact the card's response and would have to be considered in order to determine a comprehensive dose response function. Given the results of this thesis, it is most beneficial to have the two independent dosimeters coupled together, where the RadTriage cards would allow for real-time, visual dose determination and the thermoluminescent dosimeter would allow for a more robust dose determination post-exposure.

This thesis is dedicated to everyone who helped along the way. You know who you are.

I would like to extend a huge thanks to my thesis advisor, Dr. Luis Benevides, for his commitment to my growth as a student, a researcher, and a scholar.

I would also like to extend a special thanks to my parents and brother, without whom I would have never ended up where I am.

Many thanks,
Lindsay Rand

TABLE OF CONTENTS

LIST OF FIGURES

LIST OF TABLES

LIST OF EQUATIONS

CHAPTER 1: INTRODUCTION

Radiation dosimetry devices are not currently carried routinely by, or available to, a large number of designated first responders or members of the general public. This is due to the required training, funding, hardware space, and administrator knowledge needed to deploy such an endeavor. [1] Smaller, lightweight detectors that do not require user interaction, such as thermoluminescent dosimeter (TLD) badges, are most often the type of device provided to first responders, however current technology requires TLDs to be read with an annealing oven, and thus does not allow for a real-time dose estimate. For these reasons, governmental agencies that employ first responders are currently researching the suitability of colorimetric ionizing radiation (also referred to as radiochromic) dosimeters as a potential tool to provide to first responders that will not require significant hardware and training, but that will immediately and clearly indicate radiation dose exposure.

Radiochromic dosimetry has been studied since 1965 as a potential solution to fill the need for a dosimeter with high spatial resolution, but without a special analysis procedure. Since then, the study of radiochromic materials, or materials that change color in response to ionizing radiation, has evolved to include research investigating how thin films, thick films, gels, liquid solutions, and liquid-core wave-guides respond to ionizing radiation. [2] In 1998, the American Association of Physicists in Medicine (AAPM) published a seminal consensus report, AAPM 63, on the clinical use of radiochromic films to provide a standardized clinical methodology. [3] The AAPM report reviewed then-current scientific advancement in the field and provided recommendations for acceptable, standard protocols on the use of radiochromic films for dosimetry. This report included research and recommendations on proper scanning and analysis methods, in

addition to direct application of film during exposure. To date, this is still the most comprehensive report in the field of colorimetric dosimetry, and even then, only focuses on therapeutic clinical purposes and radiochromic films. It does not mention the gels and plastics that are now proliferating in the field of personnel dosimetry. [3]

Beyond the diagnostic and therapeutic clinical fields, there is growing interest in the mass production of standard radiochromic devices that are able to be used in the broader public forum by members of the public that have limited knowledge of radiological safety engineering. Such potential devices, in the form of badges, stickers, or embedded components, would offer the opportunity to provide first responders, emergency workers, and even the general public with a tool to view and measure their exposure to radiation. However, there is still research to be conducted to understand the functionality of such tools, and how standard readings can be achieved, if such readings are possible at all.

The ideal properties for such a dosimeter would include: ease of use, a standardized reading methodology to minimize false positives and negatives, and indication of dose within a certain range of ionizing radiation exposure. As first responders may be exposed to many forms of radiation, varying by radiation type, energy, and dose rate, it would also be ideal to identify a general-use radiochromic badge to respond to all forms of radiation (neutron, beta, alpha, and gamma) and dose rates with consistency. This ideal radiochromic dosimeter would also immediately indicate the associated risk of exposure in an easily understandable method, but at the same time be able to be read with a quantifiable measure post-event, allowing for more accuracy and greater granularity in assessment of the dose to determine potential health consequences.

One such dosimeter that is being considered to fit these needs is the RadTriage colorimetric dosimeter, manufactured by JP Laboratories.

In this research, we intend to verify the peer-reviewed published results that proved the efficacy of the RadTriage colorimetric dosimeter, previously known as the Self-Indicating Radiochromic Dosimeter (SIRAD), that have been published in conjunction with the manufacturer, Dr. Gordhan Patel of JP Laboratories. [4-8] Thus, for governmental agencies looking for an unbiased evaluation, this research will provide an independent, third party analysis of RadTriage. Furthermore, this research will expand the body of work on the methodology for reading RadTriage (or SIRAD) cards post-event, in a quantifiable and precise manner through the use of densitometry with a commercially available digital scanner. Beyond determining whether or not the cards are able to produce quantifiable results that can be fit with a function corresponding to exposure dose, this research will also evaluate if the RadTriage card response could reliably quantify doses below 50 mSv (the manufacture-specified threshold), using the digital scanner and densitometry methodology. Finally, this research will evaluate the effects of incident photon energy and dose rate on the RadTriage colorimetric card dose response.

Although there are currently no consensus standards for colorimetric personnel dosimeters, this research will rely upon the American National Standards Institute (ANSI) standards when relevant in establishing dose response evaluations. Specifically, this thesis will draw from testing and analysis methodology in ANSI standards for personnel dosimetry performance (ANSI Standards N13.11) and ANSI standards for accident dosimetry (ANSI Standards N13.3). [9] Through investigating the efficacy of the RadTriage detectors, informed by ANSI standards N13.11 and N13.3, this research will

examine the batch uniformity, response due to dose exposure variations (radiation energy and radiation exposure rate), and response at low doses. This research will also test a method for gathering quantifiable and precise exposure data from the RadTriage cards. In determining the ability of the cards to operate successfully with respect to these characteristics, this research will compare the sensitivity and functionality of RadTriage cards to that of TLDs, using TLDs as the gold standard comparison.

The goal of this research is to aid governmental agencies with first responders that are considering buying colorimetric dosimeters for personnel dosimetry in making a scientifically-based decision to determine the card's ability to meet specific personnel dosimetry priorities and needs. This research may also provide useful data that could be used by other agencies to satisfy personnel needs, as well as members of the general public who wish to better understand their exposure to ionizing radiation. Finally, it could also be useful for organizations that operate at the interface of radiation activities and the public to use these types of tools as trust-building opportunities. For instance, a nuclear power plant company or the government agency in charge of it, may offer to provide members of the surrounding community with RadTriage badges in order to assure transparency to the public in the work being performed and safety from accidental or unannounced exposure. Currently, such outreach efforts are limited to the distribution of potassium iodide (KI) pills to be used in case of accident exposure to ionizing radiation or information packets as delineated and mandated by the Code of Federal Regulations (10CFR) and as regulated by the Nuclear Regulatory Commission (NRC). [10]

CHAPTER 2: COLORIMETRIC DOSIMETRY BACKGROUND

History of Colorimetric Dosimeters

Any medium that changes color upon exposure to radiation can be considered a colorimetric radiation detector. Colorimetric detectors, due to their ease of readability and their general prevalence in society, are one of the oldest methods for detecting radiation. In fact, a multitude of materials can change color upon exposure to radiation, including human skin which becomes inflamed and turns red after receiving a certain threshold of exposure (called erythema). Erythema is variable by individual, thus across multiple individuals the threshold dose falls within a certain biological effect range. Other early detectors included the silver halide photographic media that was used in the discovery of x-rays by Roentgen and barium platinocyanide pastille discs that were used as early absorbed dose determiners. The drawbacks for these early and rudimentary detectors included lack of precision (varying dose thresholds) and, in the case of silver halide photographic media, specialized calibration methods and long development processes. [11]

It was the move from simple imaging and binary analysis (whether over or under a given threshold) to consistent and quantifiable coloration radiation response that required more complex materials and more in-depth research for innovation. Within the last 20 years there have been major improvements in the sensitivity to radiation and subsequent dose-related and tissue-equivalent response in modern colorimetric detectors. These improvements first led to the development of the “radiochromic” film, which has since been widely applied in the medical field due to its ability to not only detect but also image the incidence of radiation exposure. In the case of the radiochromic films, radiation exposure results in a dye formation that alters the color of the film, making a visibly noticeable change. [12] Subsequent innovation has led to colorimetric detectors

that can also visualize doses in three dimensions, including radiochromic gels and radiochromic plastics. [13] The goal of each of these types of detectors is to use a radiochromic material that responds to radiation by yielding a varying optical density. The optical density, and specifically the change in optical density before and after irradiation, can then be measured and analyzed to determine the dose to a given area in two or three dimensions. The evolution of each of these types of detectors, as well as the associated analyses methods, paved the way for radiochromic dosimeters, and the idea to use colorimetric properties to visibly indicate dose to personnel in real time.

Radiochromic Films

Radiochromic films were first designed and invented to provide high spatial resolution and weak energy dependence dose imaging of high dose gradient radiation fields. This is especially useful in the medical and clinical fields where it is important that practitioners are able to determine where the highest dose from an exposure instrument will fall incident; this includes diagnostic and therapeutic applications. The dose can then be measured by applying some function to measure the change in optical density before the irradiation and after the irradiation. Most radiochromic films have a non-linear/exponential response function to determine a dose from a change in optical density. The exponential functional form takes into account the early linear, proportional response of the detector as a function of dose, until the capacity for the detector to respond is exceeded as the radiochromic material is physically saturated at higher doses. [14]

Innovation in material science studies that led to more radio-sensitive media allowed for broader application of radiochromic films. The high detection range (10^3 to 10^6 Gy) of early radiochromic films made of media that produced triphenyl methane molecule-based particulate compounds upon exposure circumscribed their applications to

industrial food irradiation and sterilization verification processes. [15] Eventually, a more sensitive radiochromic film medium was discovered that lowered the threshold dose to 5 Gy. The new film type, utilizing the production of polymerized crystalline polyacetylenes to indicate color change, has become generally known as GAFchromic™ film, named after its manufacturer, the General Aniline and Film Corporation (Parsippany-Troys Hill, NJ), a division of ISP Technology (Wayne, NJ). [15]

The GAFchromic™ line has since developed a variety of film types to meet the needs of numerous medical applications, including diagnostic and therapeutic applications. The earliest film series, the HD-810 series, was relatively insensitive compared to modern standards, requiring a 30 Gy dose to yield an observable and measurable optical density. The one advantage of this early series was the thinness of its emulsion layer, allowing for closer proximity to the surface where the dose determination is desired. GAFchromic™'s next series, the MD-55-2, had an increased sensitivity, with a detection range between 1Gy and 100 Gy, but at the tradeoff of an extra emulsion layer, and thus increased thickness. This increased thickness can pose a problem for medical instruments with high three-dimensional dose gradients. The more recent series, and perhaps the most commonly known, is the EBT which has increased sensitivity and increased water equivalence, allowing for a more accurate read of dose with respect to tissue equivalence. Finally, the XR Emulsion-based Model allows for readings of low energy photons, which is especially useful for medical x-ray procedures. [16]

As exemplified by the variety of films that have evolved, radiochromic films can have many unique benefits that increase their usability in the medical field. One of their greatest advantages is their spatial resolution, which far surpasses other typical medical dosimeters like ion chambers and TLDs. They can also be made to image and measure x-

ray exposure far better than other devices. [14] Additionally, their ability to provide spatial resolution in response to a variety of radiation energies is especially useful in the medical field to understand where doses are being concentrated and better position patients to provide more expedient and safe treatment.[15] On the other hand, the downfall of radiochromic films compared to their contenders is a relatively higher variance in response, which can be problematic when an absolute dose, as opposed to a relative geospatial analysis, is desired. The requirement for absolute doses is becoming more prevalent in fields with increased standards required for clinical treatment and use. [17]

Radiochromic Gels

Whereas radiochromic films are limited to two-dimensional visualization of dose, radiochromic gels allow for three-dimensional visualization. This is important in many radiotherapy fields such as brachytherapy, in which doses and dose rates must be measured radially from the center of the source. Another important field of application is the comprehensive visualization of three-dimensional doses provided by external beam conformal radiation therapies, such as Intensity Modulated Radiation Therapy (IMRT), Volumetric Modulated Arc Therapy (VMAT) and Stereotactic Ablative Radiation Therapy (SABR). [18]

Radiochromic gels, although operating under the same basic principles of dose visualization through change in optical density, rely on different physical materials than do radiochromic films. Radiochromic gels use polyacrylamide gels that cross-link polymers during exposure to radiation. This is due to nuclear relaxation of gel water that causes the polymers to react, the cross-linking is visible as a change in optical density throughout the volume of medium. Radiochromic gel dosimetry has the benefits of a higher range of precision than films, due to greater statistical power achieved by added

response layers, and thus increased probability of indication, as opposed to the single layer response of films. [19, 20]

Radiochromic Plastics

Another field of study in three-dimensional dosimetry is radiochromic plastics. Similar to radiochromic gels, radiochromic plastics rely on the changing of chemical structure during exposure to radiation. However, unlike radiochromic gels, radiochromic plastics have the stabilizing substrate of polyurethane. As opposed to gels, which can be read by MRIs, Optical CTs, and X-Ray CTs, plastics can only be read by Optical CTs alone. Despite this disadvantage, one advantage of gels is that they are capable of being used much longer after initial preparation than polymer gels, which must be used within a certain window of time after preparation for a highly accurate dose. [18]

Colorimetry Densitometry

The change in optical density of the radiochromic material produced by an irradiation is measured quantitatively through densitometry analysis. Densitometry, or the measurement of the transmission, reflection, or absorbance by or through a material, principally requires some type of light source to probe the material. Different types of light sources/scanning systems have historically been used to read colorimetric dosimeters, including: spectrophotometers, scanning laser densitometers, converted infrared film densitometers, VIDAR scanners, and even flatbed scanners. [20]

The densitometry measuring system applied in this research, a flatbed scanner, has been widely studied due to its commercial availability and ease of use. The general flatbed scanner system utilizes a white light (400-700 nm wavelength spectrum) lamp. The lamp light is reflected from a film that passes through the lens of the scanner, and the image is focused into a charge-coupled device (CCD). The CCD signal is then converted

into a digital signal through measuring charge intensity. Research literature recommends systems with at least 48-bit images for color scanners (16 bits in each RGB color channel). Research literature also recommends using the scanner in reflection mode for better low-dose resolution as opposed to transmission mode (in which the lamp itself is also moving). Finally, literature recommends the conducting of two warm-up scans prior to scanning the sample, and then three subsequent scans, taking the average of the last three as the true measurement. Under these analysis methods, there is no literature to support the possibility of the scanning process iteratively changing the response indicated on the dosimeter. [21] These recommendations were all followed and incorporated in the material procurement for this research.

Analysis after scanning is conducted by comparing the optical density, measured through a standard photo analysis software (such as Photoshop™ or ImageJ™), before and after irradiation. To minimize uncertainties in readings based on time after exposure, literature sources suggest measuring the optical density between 12 and 24 hours after irradiation, as readings before 12 hours don't allow for a sufficient reaction time to be consistent and readings after 12 hours will change very little over longer periods of time. The 24-hour cap is to avoid change as a result of background dose. [20] While much effort has been made to achieve a linear fit between optical density change and dose, this is rarely achievable across a large range of doses. The predominant fits used in literature for the dose response curve are the polynomial function ($F(d) = Ad^2 + Bd + C$) and exponential function $F(d) = A (1 – e ^{(\lambda d)})$. These fits show that radiochromic dosimeters have linear responses at low doses and an exponential response at high doses; within a certain range of doses, the polynomial fit is a fair approximation, but the exponential function satisfies the boundary requirements of a plateau at higher doses. [15, 16, 17, 21]

CHAPTER 3: RADTRIAGE BACKGROUND

Basic Properties

The RadTriage dosimeter card is the latest in a family of radiochromic dosimeters produced by JP Laboratories (JP Laboratories Inc., Middlesex, NJ). Previous dosimeter cards produced by the same manufacturer, known as Self-Indicating Instant Radiation Alert Dosimeters (SIRADs), relied on similar properties but had less radiosensitivity. The RadTriage dosimeter card relies on the radiochromic polymerization of chemicals applied as a thin layer to a wallet-sized card, referred to as the emulsion layer, and is intended to be worn on a personnel badge for ease of use.

The card, shown in Figure 3.1, indicates that it is intended to be read at doses between 50 and 4000 mSv. Visual reading is performed by comparing the gray-level of the sensor strip (running horizontally in the middle of the card) directly to calibrated responses with varying optical densities positioned around the sensor strip. The card also contains a FIT indicator (false indication test) to show if the card has been tampered with or if the card has expired by a visible color change. The front of the card also indicates that the card expires two years after it is issued, after two years the sensor strip may still be responsive but, due to loss of calibration comparative to the reference boxes, the performance is no longer guaranteed by the manufacturer.

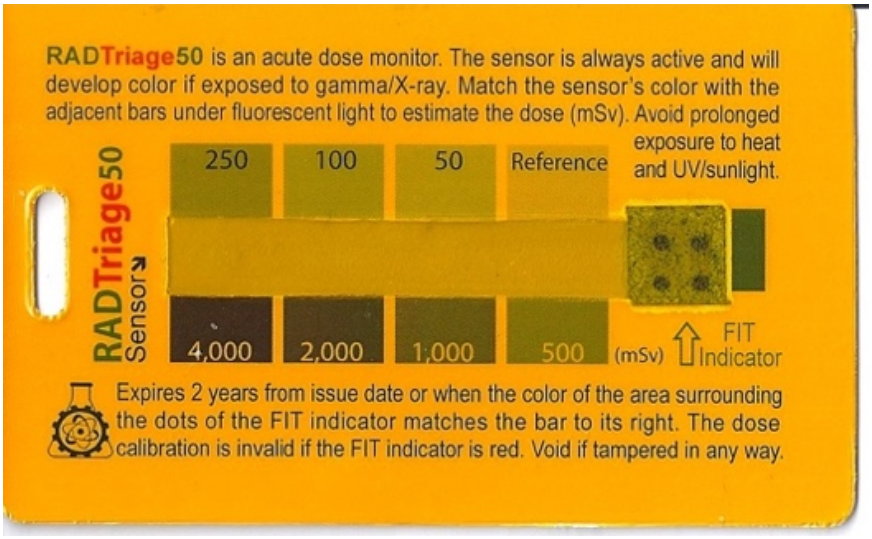

Figure 3.1: RadTriage Card Face. The front of the RadTriage card (JP Laboratories Inc., Middlesex, NJ) contains the radiation indication strip in the center, reference images surrounding the sensor strip, and a FIT indicator to show when the card has been tampered with or lost calibration.

Applications

RadTriage cards are advertised as being ideal tools to provide for individuals with minimal background knowledge on radiation detection and dosimetry, and as being ideal in situations where electronics may be compromised, or dose and necessary precaution may be immediate. This is because they indicate radiation dose instantly in a manner visible to the naked eye. They also do not rely on electronics, so they do not run out of batteries and would not be affected by an electromagnetic pulse or some other electrical interference. [5]

RadTriage cards, or their preceding SIRADs, were widely sold and distributed following the Fukushima nuclear reactor accident when many citizens were concerned about radiation exposure and wanted to verify for themselves, and monitor in real-time, any radiation they may have been exposed to. RadTriage cards have also been sold at

online marketplaces, advertising themselves as being ideal for fall-out shelter and emergency kits, as they are able to be used without access to electricity and with limited knowledge. Finally, RadTriage cards have been distributed by governments to first-responders in limited but pertinent instances. [1, 22]

Chemical Principles

The radiochromic component of RadTriage and SIRAD cards are chemical compounds called diacetylenes. Although in their native form (R' – C = C – C = C – R") diacetylenes are colorless monomers, when exposed to radiation they form polymers (generally: - (R')C – C = C – C(R") -) that are red or blue in color; in the case of the RadTriage cards used for this research, the polymers result in a blue color indication. [5] Although the diacetylenes are most sensitive to ionizing radiation, in some cases slight reaction and color change can occur in response to ultra violet (UV) radiation. To prevent against this undesired reaction as much as possible, the sensing strip is covered with a protective plastic that is polarized to allow only 1-5% of UV light to penetrate. Additionally, JP Laboratories recommends storing the cards in covered cases when not actively in use. [5] The protective plastic is yellow/orange in color and thus the blue polymer formation appears gray/green to the user post-exposure (see Figure 3.1 above).

The RadTriage cards are otherwise generally stable in ambient environments. However, exposure to extreme temperatures can impact the cards; low temperatures do not drastically affect the sensor strip, but high temperatures (exceeding 50°C) can cause premature polymerization and may indicate a false positive. A FIT indicator sits at the end of the sensor strip to indicate (through a change in color) when the card is likely to be compromised by a false positive, false negative, or loss of calibration due to UV exposure, extreme temperature effects, or expiration due to shelf-life. [5]

Radiochromic Dosimeter Literature

Prior research studies on radiochromic dosimeters, and in some cases RadTriage cards specifically, have probed a wide variety of characteristics of the radiochromic media, including the response effects related to extreme temperatures and humidity, varying gamma photon energies, and varying radiation types. The literature does not provide sufficient data on the impact of dose rate on the card reading. [23-28]

1. Temperature and Humidity Dependence

Abdel-Fattah and Miller studied the impact of humidity and temperature on radiochromic dosimeters, investigating a relative humidity range of 11-94% and a temperature range of 20-60°C. [23] Their research found that within a reasonable range of temperatures in a normal environment, 20-50°C, the dosimeter response depends very little on temperature (on the order of 0.5 to 0.25% ± 0.1% variance per °C). [23] Because they found that humidity and temperature could not be treated as independent variables, they also concluded that the same dependence and rate of fluctuation was found between 20-53% humidity. This fluctuation is due to the fact that at extremely high temperatures and humidity levels the diacetylene polymers reach a melting point and denature, causing the optical density to change and indicate a color change. Although it would be hard to shield the dosimeter from extreme environmental temperatures, Abdel-Fattah and Miller found that humidity impact can be limited by applying a seal or coating over the sensor strip; such a coating is incorporated in the RadTriage card. [23] At extremely high temperatures (exceeding 50°C, or 122°F) and with humidity change stabilized through a coating the variation in response may reach as much as10-20% difference from the expected response under standard conditions. This temperature dependence means that climate-controlled storage is important.

2. Gamma Energy Dependence

Prior research conducted by Chelminski *et. al.* and Rink *et. al.* has concluded that the response for investigated radiochromic media, GAFchromic™ EBT, is not energy dependent within the gamma energy range at doses above 1 Gy. The research groups found that at doses below 1 Gy there may be energy dependence, depending on the type of radiochromic material used in the dosimeter. For certain materials, especially radiochromic films, radiochromic dosimeters have been found to have a higher responsiveness and greater sensitivity in optical density change at lower gamma energies. This is consistent with the range of operable doses for RadTriage and the Chelminski *et. al.* conclusions. [24, 25]

3. Radiation Type Dependence

Prior research has also been conducted to determine how non-gamma radiation affects the RadTriage cards. Abegaz concluded that the cards are sensitive to beta radiation, however this research was only conducted visually using human observation and not through a more quantitative densitometry analysis. [26] Cohen *et. al.* investigated RadTriage's ability to respond to x-ray radiation using the scanning densitometry method and have found that the cards respond less sensitively, exhibiting a lower optical density change, for x-ray radiation than to gamma-ray radiation. Thus, Cohen *et. al.* concluded that the card's radiochromic material dose-response was probably calibrated with gamma radiation, making it less responsive at photon energies above and below the gamma range. [27] This is likely a feature of the radiation energy dependence discussed in the previous section. Finally, research conducted at Oregon State University by Bak concluded that the cards are not sensitive to neutron radiation, though this research was

conducted on a previous version of the RadTriage card, so the manufacturer may have corrected for this problem. [4, 28]

Standardized Reading

One major concern over the use of radiochromic materials as dosimeters is the readability of such devices from person to person; for example, inter-person visual acuity variation may interfere with reliable accounting of exposure. Furthermore, scrutiny between too many shades of grey may push the biological limits of perception by the human eye. It has been found that humans are only able to distinguish 30 shades of grey, and recognition may vary from human to human. [29] Finally, scrutiny between shades may be severely limited or altogether impossible for individuals with visual impairments, such as color blindness.

Although in the moment of an emergency, a quick and easy read for a wide range of doses may be acceptable, there would be a lot of interest post- exposure to determine more definitively what the dose received was. This concern led to the application of densitometry in analyzing and quantifying the optical density change of radiochromic materials. Such an analysis technique allows for a more precise, standardized, and reproducible method to measure the material's response based off of pixel counts provided from scans of the indicating material. As the use and types of radiochromic films have evolved and broadened, studying the best way to scan such dosimeters after exposure has become its own line of research, with many researchers postulating the best types of scanners or image processors to use for the best reading analysis. [3, 20]

Recently, Chen *et. al.* published results on how to characterize absolute dosimetry from radiochromic films using flat-bed scanners, [20] expanding upon the standard procedures provided in the AAPM 63 report [3] that are not scanner-specific. Chen *et.*

al.'s research was based on EBT3 and HDv2 films, however since the general process is to measure the absolute change in color, irrespective of the particular radiochromic media used, the procedures and findings would not be too dissimilar from RadTriage/SIRAD products and thus have been applied with success by one other research group at Oregon State University studying RadTriage cards. [28] To perform their study, Chen *et. al.* used three different types of flat-bed scanners: the EPSONV750, the EPSON 11000XL, and the EPSON 2450 produced by Epson Electronics Company (Suya, Japan). Chen *et. al.* tested measurement of the optical density change using all red, green, and blue (RGB) sensors, as well as black and white scanning. They found that there is little change across the RGB spectrum, and that measuring the entire spectrum is perfectly adequate. [20] The procedure that they used throughout testing has heavily influenced the methodology of this research.

CHAPTER 4: THERMOLUMINESCENT DOSIMETRY BACKGROUND

The thermoluminescence property of some inorganic materials when exposed to ionizing radiation has been widely employed in the use of passive radiation detectors/dosimeters, with applications in military and medical activities, as well as environmental surveillance. Dosimeters that rely on material luminescence under the application of heat, also known as thermoluminescent dosimeters (TLDs), are widely touted as the gold-standard for comparative dosimetry due to their high sensitivity, ease of use, and linear dose response. [30]

The most common TLD type used in industry is composed of lithium fluoride (LiF) in a solid crystal structure with various other elements in smaller quantities embedded in the LiF lattice to act as dopants. These lattices and dopant materials can be used to measure radiation dose due to the fact that radiation imparts energy upon the doped lattices (cut in the form of small chips) that can subsequently be read out and measured. The energy transfer from radiation to the material occurs as the radiation ionizes atoms in the TLD lattice material and creates free electrons that are trapped by the imperfections/dopants in the crystal lattice. The cards are read by heating the crystal, causing the lattice to vibrate and release trapped electrons. The released electrons drop to their original ground state and release energy in the form of light. The amount of light released at each temperature is measured using a photomultiplier tube. [31]

Within the field of TLD dosimetry, a wide variety of materials have been used as dopants to shift the response characteristics of the TLDs to meet different dosimetric needs. Effective high-Z materials such as calcium fluoride (CaF_2) and calcium sulfate ($CaSO_4$) respond with extreme sensitivity to radiation and thus are good for low-exposure needs, such as in environmental surveillance. On the other hand, high sensitivity can lead

to overresponse at low energies and can thus result in a decrease in accuracy when trying to determine the tissue equivalency of a certain dose. This setback led to the development, and wide employment across medical and military fields, of magnesium (Mg) and titanium (Ti) dopants which together, as LiF:MgTi, result in a dosimeter with a much closer tissue equivalency in exchange for a loss in sensitivity. [31, 32]

In 1978, Nakjima *et. al.* posited the idea of using LiF crystals doped with magnesium (Mg), copper (Cu), and phosphorous (P), (LiF:MCP), as a highly sensitive TLD with a close tissue equivalency. LiF:MCP is now widely favored for dosimetry due to its high sensitivity, near tissue equivalence, and linearity of dose response, making it match more common dosimetry needs than any of its predecessors were able to. Furthermore, LiF:MCP TLDs are also capable of being neutron-sensitive when enriched with Lithium (Li). [32] However, the limitations of LiF:MCP include a loss in sensitivity after overheating and an increased residual signal after repeated irradiation read cycles.[32, 33] Despite these disadvantages, and respective of the advantages, this research chose LiF:MCP TLDs to be used in comparison to the RadTriage response testing.

Glow Curve and Physical Characteristics

TLDs store energy through trapped electrons, and when heated release this energy in the form of light. To analyze a TLD chip, the intensity of this emitted light is measured using a photomultiplier tube. The process of heating the chips and measuring the light released is called “reading” the dosimeters. Depending on the dopants in the TLD, light was be released in different quantities at different temperatures. Dosimeters also must be annealed before they are next irradiated, which is the process of repeatedly heating the chips to release as many of the trapped electrons as possible, essentially erasing previous readings. [32]

The measurement of the intensity of light emitted at different temperatures is called the glow curve. The glow curve for LiF:MCP includes five major peaks, three occur at lower temperatures (70-160 °C) and two occur at higher temperatures (220 and 300 °C). The main LiF:MCP glow peak, known as peak four, used for dosimetry is seen at 220 °C. [32] Bilski *et. al.* determined the role that impurities play in producing peak four. They concluded that the height was dependent on the concentration of Cu and Mg; that the intensity of the high temperature peaks increased with increasing Mg and decreased with increasing Cu; that peak four has a step function dependence on P concentration and increases rapidly above a certain threshold concentration; and that the optimum concentration of the dopants is Mg: 0.2 mol%, P: 1.0-3.0 mol%, and Cu: 0.02-0.05 mol%. [34] Due to these concentration sensitivities, variations can occur across individual TLD chips depending on the precise chemical make-up, including specific doping concentrations that may vary across different batches and even within batches. This variation is a result of the fact that the TLDs themselves are crystals, and so definite concentrations in a certain volume of crystal cannot be guaranteed. [31]

It should also be noted that any heating beyond 270 °C can result in a decrease in sensitivity for subsequent measurements; this is the main reason why peak four, at 220°C, is the primary dosimetry peak. Chen and Stoebe explored the possible mechanisms that lead to this response and concluded that it is the result of two reactions. They concluded that the reactions involve the change in state for Cu impurities from Cu^{1+} to Cu^{2+} and that oxygen contamination in the materials can significantly impact the effects of this transition. [32, 35] Although these results did not conclusively determine how to avoid the loss in sensitivity, they did help to diminish some of the mystery surrounding the loss and implicated the possibility of future efforts to avoid the loss through material alteration.

For the purposes of this research, peak four was used and heating beyond 270 °C was avoided so as not to diminish sensitivity throughout testing (the full time-temperature profile used will be provided in the Materials and Methods chapter).

Applications

Despite the drawback of diminished sensitivity over repeated use, the advantages of LiF:MCP TLDs have led to their applications in a wide variety of practical fields, including medical, military, and environmental surveillance activities. [32] The U.S. Navy currently uses LiF:MCP dosimeters to monitor personnel dose through the use of TLD cards. Each card has four chips, with different filters to discriminate between exposures from gamma-rays, beta-rays, x-rays and neutrons. Furthermore, the Department of Defense has funded continued research into the limitations of LiF:MCP TLDs and possible solutions to such limitations. [36]

LiF:MCP is also being used in the medical field, alongside an older TLD material, LiF:MgTi. Compared to LiF:MgTi, LiF:MCP is 20 times more sensitive, but as stated, may lose its sensitivity advantage after multiple uses.[32] Although the sensitivity lost after each individual use is not significant, after a number of uses the loss in sensitivity becomes appreciable. Medical dosimetry, which has a broad variety of applications, requires a consideration for the specific need of the application at hand (i.e. greater sensitivity, better tissue equivalence, specific radiation type monitoring).

As such, depending on the requirements for the type of dosimetry, these differences may make one material more advantageous than the others. LiF:MCP has a linear-sublinear response, as compared to LiF:MgTi, which has a linear-supralinear-sublinear response. In most cases in medical dosimetery, LiF:MCP is favored because it lacks the supralinear response characteristic. [32, 38] Finally, the ability for LiF:MCP TLDs

to detect x-ray exposure has been proven, and shows greater sensitivity than LiF:MgTi TLDs which result in high uncertainty and non-linear behavior. [37] However, LiF:MgTi has the advantage of age and precedence, including the fact that it is the material that most medical standards are based off of. Yet, many researchers suspect that the sheer number and extremity of advantages in favor of LiF:MCP, as well as the rapidly growing research and innovation into the new material, make it likely that a switchover in at least a few of the applications will occur in the near term, and potentially many of the applications in the long term. [38]

Finally, TLDs are also employed in environmental exposure surveillance, as the chips are able to sit for a long period of time and collect accumulated doses. TLD materials frequently used for environmental measurements include CaF_2, LiF:MCP, and LiF:MgTi. Historically, CaF_2 was used as the highly sensitive and energy-dependent dosimeter, while LiF:MgTi was used as the tissue equivalent dosimeter. [39] However, LiF:MCP introduced the potential to consolidate these requirements into one single dosimeter material. As such, many experiments have been run to investigate the difference between LiF:MCP and its predecessors. The Nevgev nuclear research center found that LiF:MCP was able to enhance sensitivity and lower the detection limit, which ultimately resulted in a lower standard deviation in the data collected, which is more ideal for a field in which there are typically smaller sample sizes. [39]

Similar to how the different types of TLDs have various advantages and disadvantages, there are likely to be even more extreme advantages and disadvantages between TLDs and radiochromic dosimeters. As this research compares the responses of the two types of dosimeters, it will attempt to delineate the strengths and weaknesses that would be important depending on the different uses the dosimeters may be applied to.

CHAPTER 5: MATERIALS AND METHODS

This research was conducted using a radiation range at the Naval Surface Warfare Center, Carderock Division (NSWCCD) in West Bethesda for TLD and RadTriage sample irradiations. Equipment at NSWCCD was also used to read and anneal the TLD chips. An off-site digital scanner was used to scan and read the RadTriage cards after irradiation. Each test followed the same routine which will be presented in this section: sample preparation and irradiation, TLD chip reading and annealing, RadTriage scanning, and RadTriage analysis. Each dose and parameter test underwent the steps at the same timeframe (including time between preparing and irradiating the samples and time between irradiating and reading the samples) to ensure consistency in any possible time-related effects, such as time between irradiation and TLD annealing and time between irradiation and RadTriage scanning.

Sample Irradiation

In order to consistently compare TLD and RadTriage responses, the two sets of materials were irradiated simultaneously for each test. Harshaw TLD-700H series TLD chips, manufactured by ThermoScientific (Waltham, MA) were used in conducting this research. This series of TLD chips are composed of lithium fluoride crystal doped with magnesium, copper, and phosphorous (LiF:MCP), and have a standard 3.2 mm diameter and a 0.38 mm thickness. A total of 86 TLD chips were initially evaluated, but only a smaller group of 30 TLD chips were chosen to be testing samples; the selection criteria and procedure to choose these 30 chips is provided in Appendix B. For the RadTriage card samples, 150 RadTriage cards were provided by Dr. Gordhan Patel of JP Laboratories (Middlesex, NJ). Because the cards are manufactured for one-time use only, new cards had to be used for each test.

All tests were conducted at a Radiation Technology Group laboratory at the NSWCCD. Between the irradiations, the TLD chips were stored in plastic microtubules at the NSWCCD facility and the RadTriage cards were stored in a sealed filing cabinet within two sets of insulated envelopes to limit exposure to UV radiation. All samples were stored in climate-controlled facilities that were kept at room temperature.

All irradiations were provided by using a Hopewell Designs (Alpharetta, GA) Model GC-60 Gamma Beam Irradiator (GC-60), shown in Figure 5.1. The irradiator is positioned in front of a calibrated moveable track to allow for easy measurement of the distance between the irradiator source and any position along the track. With this irradiator, a Cs-137 source and a Co-60 source were used to provide the gamma irradiations.

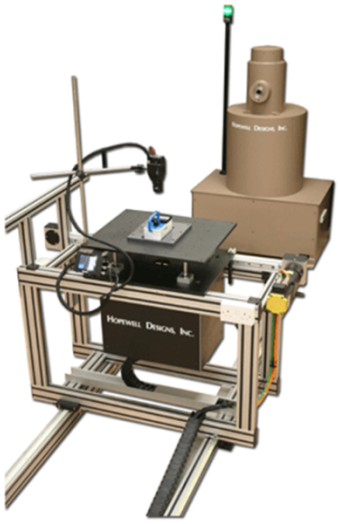

Fig. 5.1: Hopewell Designs GC-60 Gamma Beam Irradiator. The calibrated track and moveable table setup are also shown in the figure in front of the GC-60. This image was taken from publicly distributed documents at Hopewell Designs Inc.™ (Alpharetta, GA).

Before each test was conducted, an Exradian (Middleton, WI) A5 spherical ionization chamber was used to acquire an exposure rate calibration for the specific

position along the moveable track at which the test would be conducted. The ionization chamber is traceable to the National Institute of Standards and Technology (NIST) and was last calibrated in June 2018.

Once the ion chamber was set up in the correct track position for the associated test, shown in Figure 5.2, the manufacturer-specified bias voltage was applied, and three one-minute irradiations were conducted. An average was taken of the three irradiation measurements to get an associated calibrated dose rate for the specific position along the track; the three measurements were also used to determine a standard deviation in the calibrated dose rate. A calibrated dose rate for each test was found using this method to ensure that the irradiations for the test were corrected for variations in temperature and pressure throughout the duration of the research testing, and to ensure that a calibrated dose was found at the specific location along the irradiation track required for testing. More information about the use of ionization chambers for calibration and the data from each of the calibrations performed is provided in Appendix A.

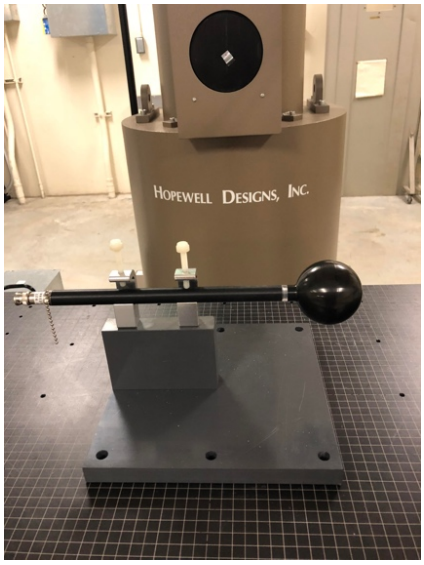

Figure 5.2: Ion Chamber Calibration Setup. The GC-60 Hopewell Designs (Alpharetta, GA) is shown behind the A5 ion chamber used for irradiation calibration. Photo taken at NSWCCD.

Because the dose rate calculated from the ionization chamber had the units mR/min, the average was converted to dose rate in the form of mSv/min, to match the mSv units shown on the RadTriage cards. This rate was divided by 60 to get mSv/s and multiplied by 1.21 (found in ANSI Standards 13.11) to get the deep dose equivalent, accounting for the backscatter from a phantom placed behind the dosimeters during the exposure. This calibrated deep dose equivalent rate was used to determine the number of seconds required to provide the test-specific dose to the dosimeters. The conversion used to get the appropriate number of seconds for each trial is provided below:

Equation 5.1: $$Irradiation\ Time\ (s) = \left(\frac{Desired\ Dose\ (mSv)}{Ion\ Chamber\ Calibrated\ Dose\ Rate\left(\frac{mSv}{s}\right)}\right).$$

After the exposure calibration was performed for a specific test and the time required for the irradiation was calculated, 10 LiF:MCP TLD chips in a 100-slot acrylic holder and seven RadTriage cards were fastened to a 30 cm high, 30 cm wide, and 15 cm thick polymethyl metacrylate (PMMA) acrylic slab phantom using hook-and-loop fastener adhesive. This setup is shown in Figure 5.3. A centering laser was used to ensure that the gamma radiation beam would fall isocenter to the setup. The same isocenter position was used for each test, the TLD chips were consistently placed in the same wells, and the cards were placed in the same locations on the phantom and numbered throughout all testing. By numbering the cards, systematic differences based on card position on the phantom could be tested. The cards and TLDs were uniformly exposed under this setup. The time at the end of the exposure was recorded for the sake of limiting uncertainty in the amount of time between exposure and reading of the chips and cards.

Figure 5.3: Phantom Setup with TLD Chips and RadTriage Cards. The setup for the TLD chips and RadTriage cards (JP Laboratories, Middlesex, NJ) that was used for each irradiation trial is shown. The cards and chips were fastened to an acrylic phantom. The chips were always placed in the same positions, and the cards were numbered based on position for every trial to keep track of any possible position-based differences. Photo taken at NSWCCD.

Annealing and Reading the TLD Chips

TLD chips were used along with the RadTriage cards in this testing in order to provide a standard for comparison. Specifically, LiF:MCP chips were used as they have a high tissue equivalency and are one of the most standard chips available.[32] The TLD chip reading and annealing for this research was conducted at NSWCCD using a Harshaw (Waltham, MA) QS Bicron Model 3500 Thermoluminescence Manual Chip Reader (shown in Figure 5.4), supplied by nitrogen gas to suppress the infrared signal of heating the chips using a planchet heater. WINDOWS Reader Evaluation and Management System (WinREMS^{TM}) software was used to read the resulting photomultiplier tube spectra of light intensity emitted per temperature increment.

Figure 5.4: Harshaw QS Bicron 3500 Manual Chip Reader. This is an image of the same system used to read the TLD chips in this research. The image was taken from publicly distributed images at ThermoScientific (Waltham, MA).

An initial test was conducted on the entire LiF:MCP TLD population available at the facility. This test allowed for the determination of a population average and reader calibration factor for the entire group of chips, as well as individual relative responses for each of the chips. The methodology for this analysis, as well as the data for each of the chips and the population as a whole, is outlined in Appendix B and follows the procedures developed by Moscovitch *et. al.*. [31]

From this data, 30 chips were selected based on the similarity in their responses. This set of 30 chips was divided into three groups of 10, to allow for up to three shots to be taken before chips had to be read. While it would have been most ideal to conduct every test with the same group of chips each time, time constraints at the lab range made this an unviable option. Furthermore, by conducting an initial population and relative chip response calculation, each of the chips was able to be given an element correction

factor, ECF, to standardize its response to the entire 30 chip population. These were used to create a group correction factor, GCF, for each of the three groups of 10 chips, and every time the chip results were analyzed, the GCF was used to standardize the group average response to the total population average to ensure that there was no TLD-related difference between the three groups used for testing that would result in different test readings.

Prior to each exposure, TLD chips were annealed on the day of the exposure to below 3 nanocoulombs. The time-temperature profile (TTP) that the chips were annealed and read at included an acquisition range of 0 to 260 °C at a rate of 15 °C/sec, based off of recommendations from previous research about the ideal TTP for LiF:MCP TLD chips analyzing peak four. Annealing was performed before each test to ensure uniformity across testing and to reduce the effects of background radiation exposure between testing. After annealing, the chips were set to cool for at least thirty minutes before the test was conducted to ensure the same thermoluminescence sensitivity across testing. [32] Ten chips were used along with each set of cards in order to increase the statistical strength of the results, verified using the analysis of variance (ANOVA) statistical model.

TLD chips were read at NSWCCD starting within one hour of the end of the exposure time. It should be noted, that in some cases each TLD chip took several minutes to read, so at times the timespan between irradiation and reading slightly exceeded one hour. However, in annealing the chips between the days of the research, is was found that chips would accrue an average of 0.28 nanocoulombs per day due to background radiation. Thus, the amount of background radiation would have only varied by 0.03 nanocoulombs for a one-hour period and thus would have been negligible compared to the levels that were found due to the radiation exposure (on the order of microcoulombs).

After TLD chips were read, an average response value was calculated for the set of chips, as well as a standard deviation. Standard deviations were monitored throughout testing to ensure there were no major inconsistencies in the reading or annealing processes, and to ensure the integrity of the chips was not compromised. The TLD curve shape was monitored to ensure there were no serious abnormalities, which would have indicated possible card contamination. Additionally, reference light and photomultiplier noise tests were conducted after every 10 readings to ensure that the photomultiplier tube was operating with stability at a known reference light emission (the reference light test) and that dark current in the absence of light was minimal (the photomultiplier tube noise test). This testing frequency, after every 10 reads, was recommended by the manufacturer, ThermoScientific – Harshaw. These results were monitored to ensure that there was no degradation of the reading instrument, and the results, as well as more information about the tests are provided in Appendix C.

Reading the RadTriage Cards

RadTriage cards were read using an HP (Palo Alto, CA) OfficeJet 6500 Wireless printer/scanner, which has a 2400 dpi optical resolution to match the suggested range of resolutions that both the ImageJ software provider (NIH, Bethesda, MD) recommends and that prior research recommends for densitometry analysis. A scanning template was made using cardstock paper and a ruler to sketch out a specific location to attach the card to the paper, to be placed on the scanner, to ensure consistency in the placement of the RadTriage card on the scanner. RadTriage cards were scanned one at a time, with each card placed in exactly the same scanner location, as demarcated by the template.

The cards were each scanned five times. This was recommended by the literature review to allow the first two scans to serve as warm-ups for the scanner light and the last

three to be used to determine an average densitometry value. [21] However, it should be noted that the veracity of the purported need for warm-up scans was tested in this research by measuring the value for the first two scans and using a T-test to determine if there was a difference of means; no significant difference was found. The results of this test, contrary to previous research, could have been the result of a difference in the properties of the films tested or a mechanical difference in the scanner used. Regardless, for consistency sake, only the third, fourth, and fifth scans were used to determine a densitometry average, henceforth called pixel density (P(D)).

The P(D) of the sensor strip on each card was determined through analyzing the scanned images with ImageJ software provided by the National Institute of Health (NIH). ImageJ is a publicly available, general-purpose imaging tool that has been applied for the purpose of densitometry analyses throughout multiple fields of research.

Nearly the entire RadTriage card colorimetric sensor strip was used for the region of interest (ROI) in the densitometry ImageJ analysis. This decision was made with the purpose of avoiding bias against fade by selecting certain regions of the strip. This same region was selected for every card, as allowed for by pre-set selection definitions in the ImageJ software. The standard deviation for each individual reading, as well as the P(D) reading itself, was recorded as provided by ImageJ software analysis prompt. The user interface setup is shown in Figure 5.5. The ROI P(D) standard deviation, though not the standard deviation used in the optical density calculation, served as a good indication of whether or not fade was observed. As the ROI was increased, the standard deviation would increase at interfaces between the sensor strip and the card itself. This increase in standard deviation was used to determine the optimum sensor strip ROI of 49,600 pixels,

this ROI allowed for the largest sensor strip area to be measured without increasing the standard deviation through extending beyond the sensor strip and onto the card itself.

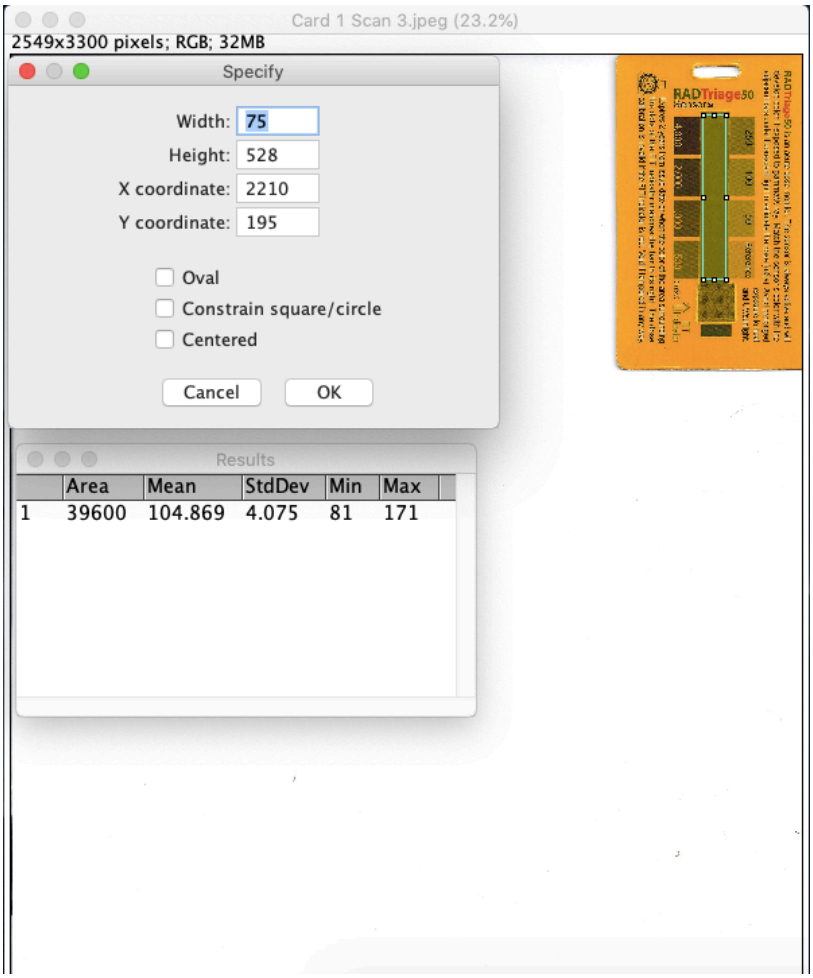

Figure 5.5: ImageJ Software Interface. The RadTriage card scans (JP Laboratories, Middlesex, NJ) were analyzed using ImageJ software from NIH (Bethesda, MD). The same ROI was specified each time to ensure consistency, shown as a green box in the upper right corner.

Just as the reference light and photomultiplier noise readings were taken for every 10 readings of the TLD chips, a similar ImageJ mean RGB value was calculated on the white screen for every set of readings, to ensure that the lightbulb of the scanner was not losing its luminosity throughout the series of tests. These results are provided in Appendix D.

For each card, the three scans following the two warm up scans were analyzed to get three scan pixel densities, henceforth called $P(D)_S$, per card. The three $P(D)_S$ per card were used to determine one average card pixel density, henceforth called $P(D)_C$. The $P(D)_C$ for all of the cards used in a specific testing group were used to calculate an average pixel density for the entire test group, henceforth called $P(D)_G$. Along with the series of scan, card, and group P(D) averages, standard deviations, σ, were determined using the same method but based on the standard deviation in pixel density provided by the ImageJ software. The pixel density values are defined below for clarity sake:

Equations 5.2.A − C

$$Scan\ pixel\ density: P(D)_s = P(D)\ over\ ROI\ for\ a\ single\ scan\ of\ a\ card$$

$$Card\ pixel\ density: P(D)_C = \frac{\sum_{i=1}^{3} P(D)_S}{3}\ (ave. P(D)\ of\ the\ three\ scans\ per\ card)$$

$$Group\ pixel\ density: P(D)_G = \frac{\sum_{i=1}^{7} P(D)_C}{7}\ (ave. P(D)\ of\ all\ cards\ per\ group).$$

It should be noted that the cards were not able to be read immediately after the tests, as the TLD chips had to be read at NSWCCD and the cards were scanned at a different location. The time that each reading was performed was recorded though, and all readings were able to be performed between 20-24 hours after the exposure time; this is within the time frame recommended by previous research using densitometry scanning analysis with radiochromic media. [21] This time frame limits the amount of background radiation accumulation, while at the same time allowing for nearly all of the chemical reaction and polymerization to occur. For reference, 2-3 mSv per year is the generally

accepted effective dose from background radiation, which would equate to less than a 0.01 mSv background accumulation between the time of the irradiation and the scan. [31]

Tests Performed

Each test was performed using nearly the exact procedure described above, though slight variations will be discussed in this section. Table 5.1 at the end of the section summarizes all of the tests performed and the variable parameter information.

In total, there were six baseline tests performed to measure the card's functionality across the range of doses specified on the RadTriage card (50-4000 mSv). All but the 4000 mSv test were performed; the 4000 mSv test could not be performed due to the fact that it would have required overnight testing at NSWCCD. These tests alone were intended to independently verify the efficacy of the cards.

There were also four tests performed below the baseline dose range on the card. These included tests at doses decreasing in increments of 10 mSv from 50 mSv to 0 mSv. These tests were all performed at a distance of 100 centimeters away from the irradiator, with the Cs-137 source; the only variation for each of these tests was the amount of time the exposure ran for (to provide the different dose).

Additionally, a total of three dose rate tests were performed to determine if the card responses vary as a function of dose rate. Again, the exposures were provided with the Cs-137 source, however for these tests the distance between the phantom holding the dosimeters and the irradiator was varied in order to provide different dose rates. The ionization chamber was used to get a precise, calibrated dose rate at each distance. The same total dose was provided for each of these groups.

Finally, a total of three gamma-ray energy tests were conducted to determine if the energy of the gamma photons would impact the response of the cards. Here, the

distance between the samples and the source remained 100 centimeters, but a Co-60 source was used to provide the dose to the dosimeters being tested. Again, the ionization chamber was used to find a calibrated dose rate for the source. The doses provided were 50 mSv, 100 mSv, and 250 mSv, these were to be compared to the three lowest baseline doses using the Cs-137 source.

Table 5.1: Testing Set-up Parameters

Test	Dose (mSv)	Source	Dist. (Cm)	Calibrated Deep Dose Eq. (mSv/hr)	Exposure Time (s)
Baseline-1	2,000	Cs-137	100	667.68	10784
Baseline-2	1,000	Cs-137	100	671.79	5358.8
Baseline-3	500	Cs-137	100	667.43	2696.9
Baseline-4	250	Cs-137	100	673.24	1336.4
Baseline-5	100	Cs-137	100	667.43	539.4
Baseline-6	50	Cs-137	100	667.43	269.7
Below Baseline-1	40	Cs-137	100	671.79	214.4
Below Baseline-2	30	Cs-137	100	671.79	160.8
Below Baseline-3	20	Cs-137	100	671.79	107.2
Below Baseline-4	10	Cs-137	100	671.79	53.6
Dose Rate 1	100	Cs-137	100	667.43	539.4
Dose Rate 2	100	Cs-137	150	297.66	1209.4
Dose Rate 3	100	Cs-137	250	106.70	3373.9
Co60-1	250	Co-60	100	485.69	1853.0
Co60-2	100	Co-60	100	485.69	741.2
Co60-3	50	Co-60	100	485.69	370.6

This table shows the tests that were conducted and the parameters for each test, including the source used in the testing, the distance from the source, the calibrated deep dose equivalent (found using the ionization chamber), and the total exposure time (calculated based on the calibrated deep dose equivalent).

CHAPTER 6: RESULTS

The results from testing are divided into four main sections: response at the manufacturer specified dose range, response at the low dose range (below the manufacturer specified range), response variability based on dose rate, and response variability based on gamma energy. A data summary for both the RadTriage cards and TLD chips will be provided, as well as data visualization when appropriate.

Response within Manufacturer Specified Range

The range of doses tested at the same distance (same dose rate), and with the same source, were based on the doses listed on the card (50 mSv to 4000 mSv). The maximum dose achieved for this setup was 2000 mSv. The full range of shots tested with the Cs-137 source at a distance of d = 100 cm is provided in Table 6.1 below.

Table 6.1 lists the dose for each of the trials, as well as the group pixel density, $P(D)_G$, the group standard deviation, $\sigma_{P(D)G}$, the change in group optical density, ΔOD_G, the mean TLD response (taken as measured charge) per group, Q_G, TLD standard deviation, σ_{QG}, and the dose standard deviation. The $P(D)_G$ has already been defined as the pixel density for the group of cards in a given test. The ΔOD_G was then calculated by subtracting the $P(D)_G$ for a given test from the $P(D)_B$ or the background average pixel density. This was the average pixel density for 10 cards that had not been irradiated, and thus served as background samples. Thus, ΔOD_G was calculated as:

$$\textbf{Equation 6.1} \quad \Delta OD_G = P(D)_B - P(D)_G.$$

The standard deviations listed are the standard deviations for each of the sets of cards (7 cards) and chips (10 chips). The TLD mean, Q_G, is slightly adjusted based on

the group ECFs to ensure consistency across sets; this was just a multiplication of the average times the group ECF which can be found in Appendix B. Depending on the set and the group ECF, ECF_G, a standardized mean reading would be achieved by multiplying the group mean by the ECF_G. Finally, the chip and card errors, propagated based on the calculations performed, are listed, as well as the error propagated from the standard deviation in the ion chamber dose calibration. These calculations were performed based on the statistical methodology presented in Knoll. [31]

The standard deviation for the group P(D) was calculated using the standard deviations for each of the means of the card scans:

$$\textbf{Equation 6.2} \quad \sigma_{P(D)G} = \sqrt{\frac{\sigma_{C1}^2+\sigma_{C2}^2+\sigma_{C3}^2+\sigma_{C4}^2+\sigma_{C5}^2+\sigma_{C6}^2+\sigma_{C7}^2}{7}}.$$

The ΔOD_G standard deviation was calculated using error propagation to weight the standard deviations of the two factors contributing to ΔOD_G, the $P(D)_G$ and the baseline $P(D)_B$, or the P(D) with no irradiation. This was based off of the error propagation process for the subtraction of one value from another:

$$\textbf{Equation 6.3} \quad \sigma_{\Delta OD(G)} = \sqrt{\left(\frac{\partial \Delta OD}{\partial P(D)_B}\right)^2 \sigma_{P(D)B}^2 + \left(\frac{\partial \Delta OD}{\partial P(D)_G}\right)^2 \sigma_{P(D)G}^2} = \sqrt{\sigma_{P(D)B}^2 + \sigma_{P(D)G}^2}.$$

Finally, the TLD standard deviation was calculated using error propagation to weight the standard deviations of the TLD mean response and the TLD ECF. This was based off of error propagation for the multiplication of two values:

Equation 6.4 $\sigma_{QG-corrected} = \sqrt{\left(\frac{\sigma_{QG}}{QG}\right)^2 + \left(\frac{\sigma_{ECF}}{ECF}\right)^2}$.

Table 6.1: Summary Table of Results for 0-2000 mSv Doses							
Dose (mSv)	**σ Dose**	**$P(D)_G$**	**σ P(D)G**	**ΔOD_G**	$\sigma_{\Delta OD(G)}$	**$Q_{G\text{-}Corrected}$ (μC)**	**$\sigma_{QG\text{-}C}$**
0[1]	0.00	139.15	3.86	0.00	5.46	--	--
10	0.58	137.25	3.68	1.91	5.33	0.90	0.10
20	0.58	136.56	2.12	2.59	4.41	1.81	0.23
30	0.58	133.77	2.51	5.38	4.61	2.75	0.33
40	0.58	132.37	1.96	6.78	4.33	3.71	0.48
50	2.52	129.69	2.77	9.47	4.75	4.04	0.74
100	2.52	123.11	2.74	16.04	4.74	9.17	1.29
250	3.51	104.98	2.86	34.17	4.81	23.79	2.12
500	2.52	85.22	2.64	53.93	4.68	46.20	8.04
1000	0.58	68.38	2.59	70.78	4.65	82.96	27.82
2000	1.53	50.05	1.13	89.10	4.03	193.45	22.03

This table shows the responses for both the cards ($P(D)_G$) and the chips ($Q_{G\text{-}Corrected}$) at each of the doses tested. The table also shows the standard deviation for card and chip readings, as well as the card response as a difference between the card mean at a dose and the card mean with no dose (ΔOD_G).

The observed card response and error values are plotted in Figure 6.1. The data points are fit with an exponential function, $\Delta OD_G(D)=A*(1-\exp(-\ln(2)*D/B)$, which was suggested by the literature review. [20-25] This fit indicates that the cards respond with rapid change at lower doses but that the response begins to taper off at much higher doses. This is consistent with the knowledge that for radiochromic dosimeters there is usually a leveling off at some point at which the polymerization reaction is saturated and

[1] This is the background reading for the RadTriage cards used as the baseline in comparison to the color change after irradiation. The RadTriage cards were read with no irradiation; the TLD chips were not read at a dose of 0 because their absolute response is not based on a comparison.

the material can no longer polymerize as rapidly in response to each additional unit change of radiation. The fit was tested using residual analysis and chi square testing, for which a chi^2 P-value of 0.998 was found, which is fairly high and suggests a high probability of fit for the function that was created.

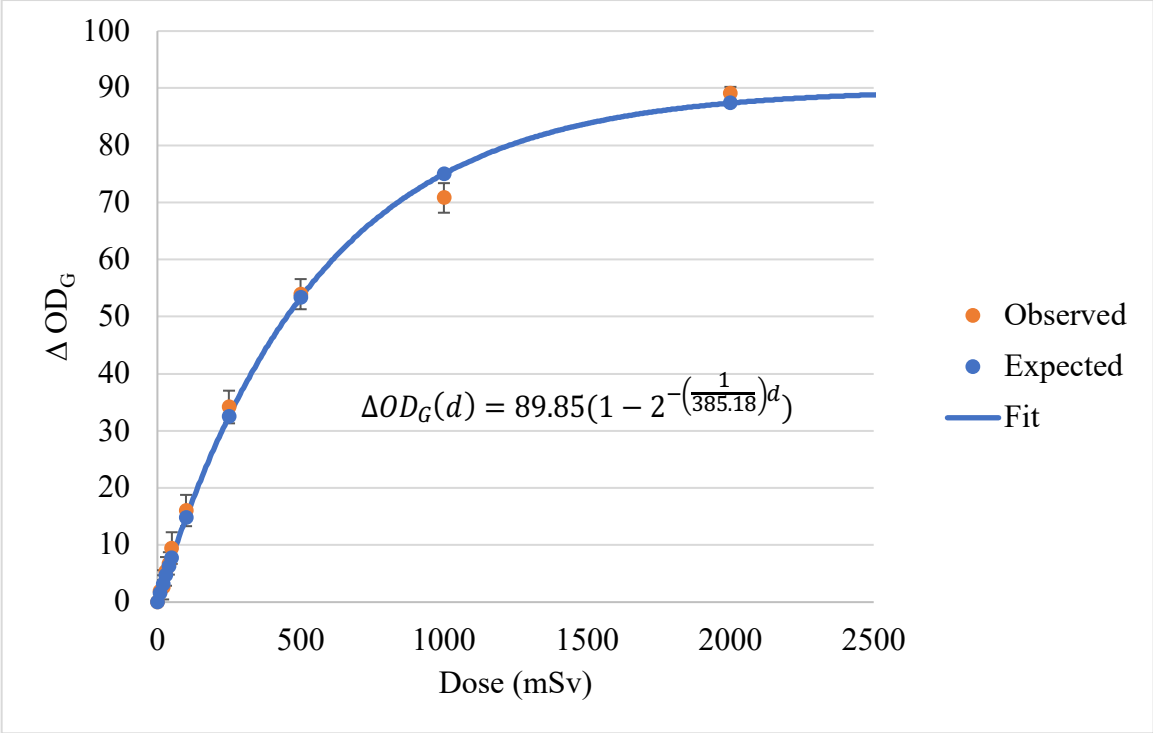

Figure 6.1: RadTriage Response as a Function of Dose. The observed response is plotted with vertical error bars indicating variation in response among cards and horizontal error bars, which are too small to be visible, indicating variation in dose based on initial calibration analyses. An exponential fit is also plotted with the data. The fit had a chi^2 P-value of 0.998 which suggests very little residuals in the difference between the observed values and the values expected based on the fit function. The function for the fit is also shown; the associated error for the terms are 89.85+/-2.05 and 385.18 +/- 35.7.

The TLD values and errors are shown in Figure 6.2. The data is fit with a linear function, as predicted by previous research, [32] and is consistent with the initial population calculation analyses conducted, in Appendix A. The R^2 value for the TLD

chips is 0.996. The response for the TLD chip groups, Q_G, is given in microcoulombs and indicates the average response for each of the groups at a specific dose.

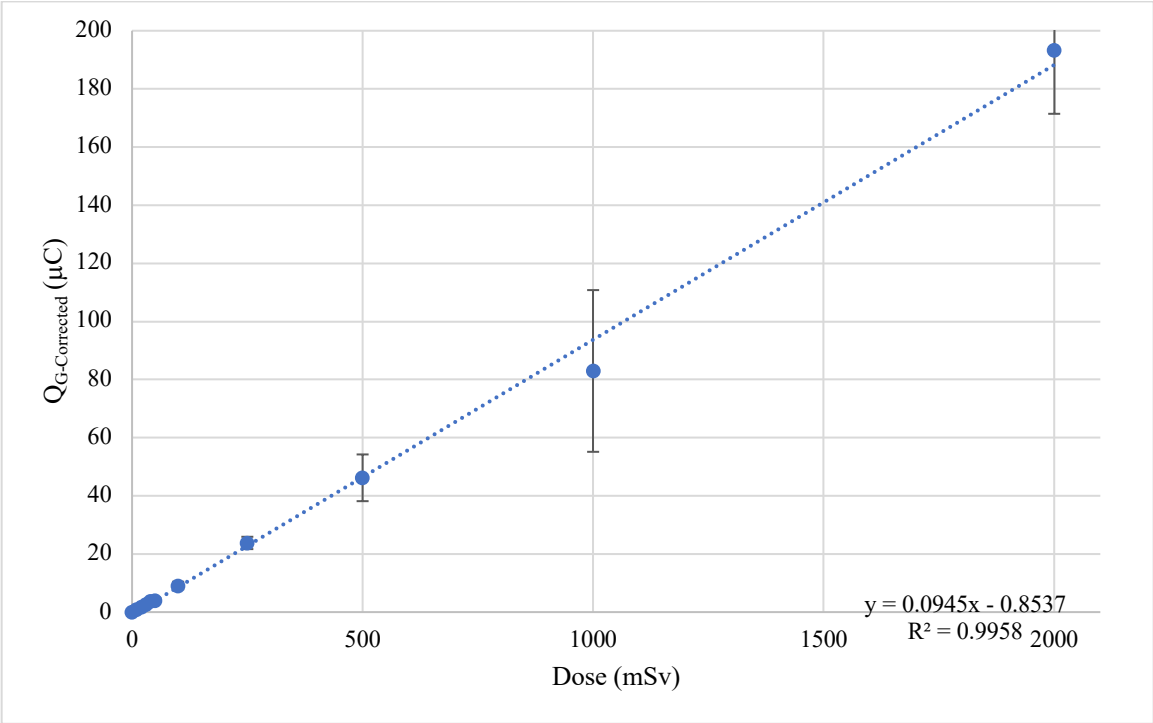

Figure 6.2: TLD Response as a Function of Dose. The observed TLD response is plotted with vertical error bars indicating variation in response among the TLD chips and horizontal error bars, which are too small to be visible, indicating variation in dose based on initial calibration analyses. Errors in the linear equation were calculated to be +/- 0.09 for the slope term and +/- 0.29 for the intercept term.

Plotting the experimental dose responses allowed for visual determination of the functional form for each response curve. The two forms identified were exponential for RadTriage, $\beta(1 - e^{\lambda d})$, and linear for TLD, Md – B. The RadTriage constants, β and λ, fit the response curve for the background response, β , and the deterioration rate of the polymers, λ. The TLD constants fit the response curve for null reading, B, and the response rate as a function of dose, M. The values for these constants were optimized using chi-square testing to minimize the residuals between the observed and predicted

values. Chi-square was also used to find the associated error by adjusting terms until the chi-square value changed by +/-1. Residual testing was plotted to check the fit for RadTriage; residual plots are found in Appendix E and the forms and fits are written as:

$$\textbf{Equation 6.5.A} \quad RadTriage\ Functional\ Form: \Delta OD_G(\mathrm{d}) = \beta(1 - e^{\lambda d}),$$

$$\textbf{Equation 6.5.A} \quad RadTriage\ Fit: \Delta OD_G(d) = 89.85(1 - 2^{-\left(\frac{1}{385.18}\right)d}),$$

$$\textbf{Equation 6.6.A} \quad TLD\ Functional\ Form: Q(d) = M(d) - B, \text{ and}$$

$$\textbf{Equation 6.6.B} \quad TLD\ Fit: Q_{G-corrected} = .0945(d) - 0.8537.$$

Response at Low Doses

The RadTriage cards were also tested at doses below their specified range in order to determine if lower doses could be detected using the densitometry scanning analysis method, even if not visible to the naked eye. The RadTriage cards were tested at doses decreasing in increments of 10 mSv from the lowest specified dose, 50 mSv. The resulting data is provided in the previous section, in Table 6.1. The results are plotted in Figure 6.3. As was suggested by the colorimetric dosimeter literature review, at lower doses the cards could be approximated by a linear response function, as the pigment formation changes directly as a function of dose. This is still able to be accounted for in our full-range dose-response function, $\Delta OD_G(D)=A*(1-\exp(-\ln(2)*D/B)$, as well.

However, it should be noted that the standard deviations, propagated in the same method as in the previous section, is relatively large compared to the incremental changes between the responses, and could be likely to skew the data for analysis with an individual card. Again, the horizontal error bars represent the uncertainty in the dose based off of the ionization chamber calibration standard deviation. The TLD response is also plotted, in Figure 6.4, and follows a linear trend. Both cards have R^2 values that indicate significant correlation ($R^2 > 0.97$).

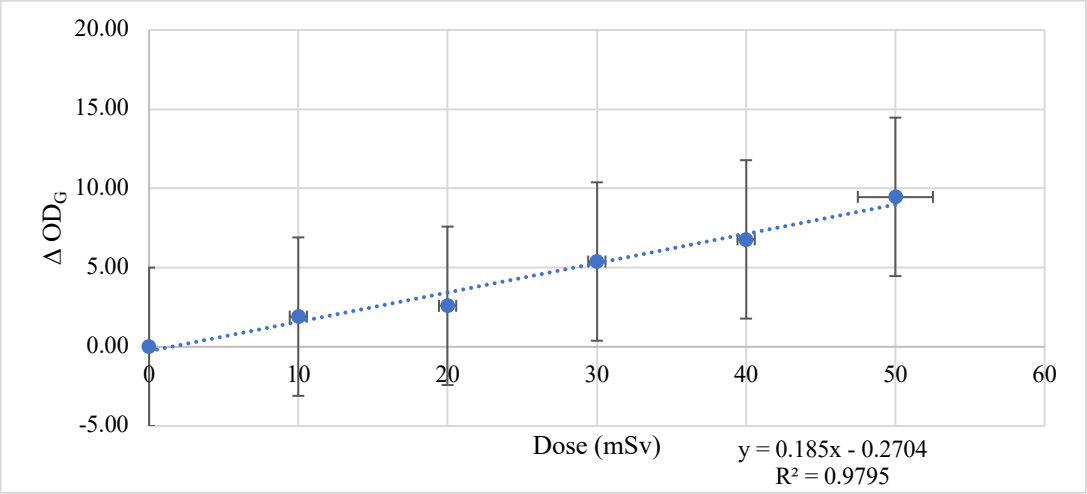

Figure 6.3: RadTriage Response at Low Doses. The observed RadTriage response follows a linear trend and has error bars that suggest considerable uncertainty for one card alone. Vertical error bars are calculated based off the standard deviation in card readings; horizontal error bars, barely visible, are calculated from the calibrated dose standard deviation. Errors in the linear equation were calculated to be +/- 0.05 for the slope term and +/- 0.03 for the intercept term.

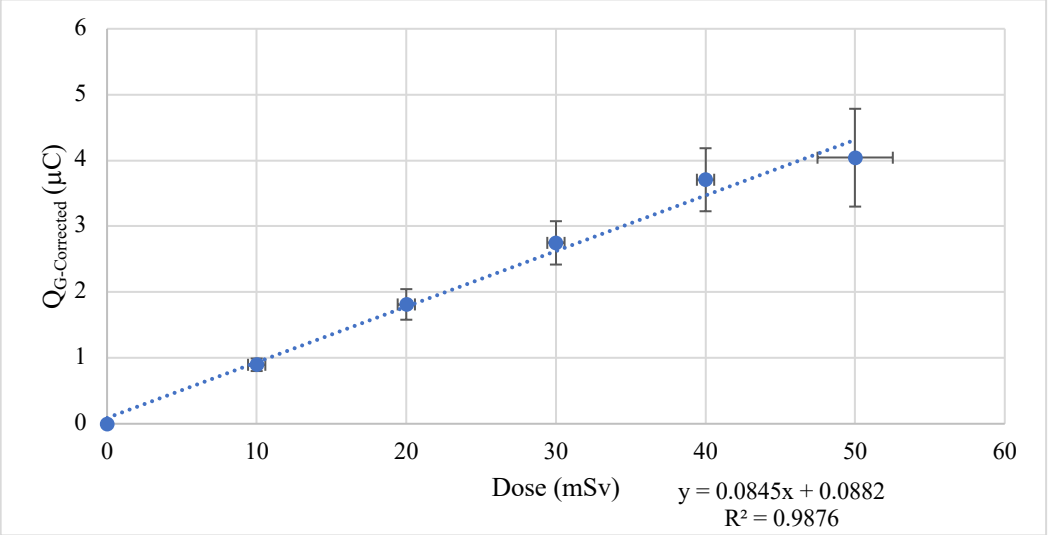

Figure 6.4: TLD Response at Low Doses. The observed TLD response follows a linear trend. Vertical error bars are calculated based off the standard deviation in chip readings; horizontal error bars, barely visible, are calculated from the calibrated dose standard deviation. Errors in the linear equation were calculated to be +/- 0.44 for the slope term and +/- 0.20 for the intercept term.

Response to Dose Rate

Response as a function of dose rate was tested using three different dose rates, accomplished by adjusting the distance between the source and the dosimeters. Ten cards were tested for each of the distances to provide greater statistical certainty given the fewer number of observations. Three dose rates were tested: 667.43 mSv/hr (100 cm), 297.66 mSv/hr (150 cm), and 106.7 mSv/hr (250 cm). The results for the RadTriage cards are shown in Figure 6.5, where they are compared to the TLD chip responses. From the graph, it can be seen that RadTriage cards have a greater absolute difference in response as a function of dose rate than do the TLD chips (a -20% change for RadTriage compared to a +11% change for TLD) and the responses are directionally different. The vertical error bars on the chart also show that the RadTriage cards had a greater deviation in responses than did the TLD chips. Once again, the horizontal error bars indicate the uncertainty in the provided dose based off of the ionization chamber calibration.

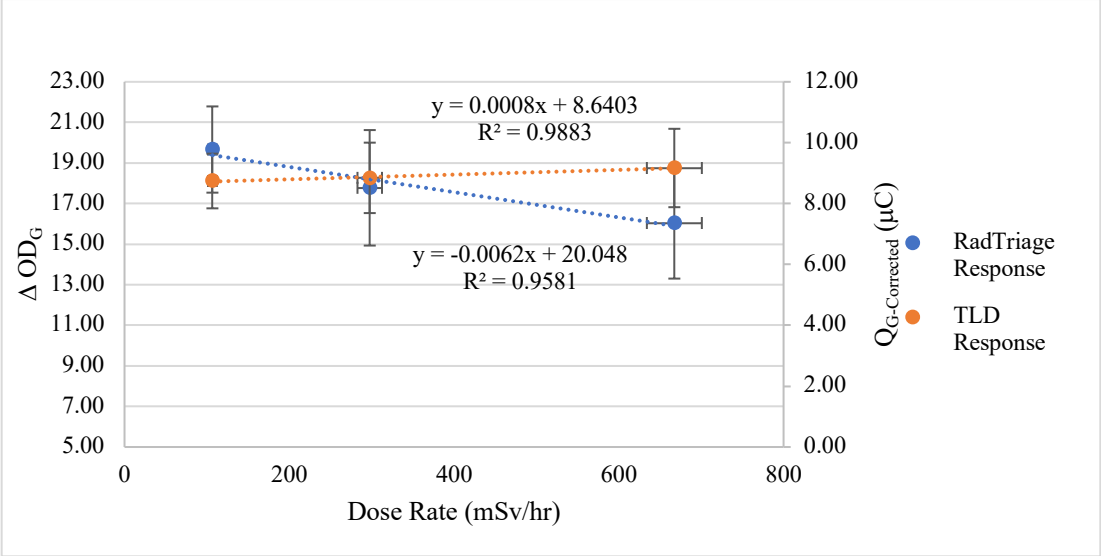

Figure 6.5: TLD and RadTriage Responses as Functions of Dose Rate. TLD and RadTriage sets each received the same dose but at different dose rates (differing by distance from the source). Vertical error bars indicate standard deviation in responses and horizontal error bars indicate standard deviation in the dose provided.

Response to Gamma Energy

Response as a function of gamma energy was tested using two different gamma sources, Cs-137 with a gamma energy of 662 KeV and Co-60 with two gamma energies nearly double that of Cs-137: 1173 and 1333 KeV. This variation in gamma energy was used to test whether or not there could be a change in response based on the gamma energy of the source. This was tested at three different doses, 50 mSv, 100 mSv, and 250 mSv. The results for the RadTriage cards are shown in Figure 6.6. The chart also includes horizontal error bars indicating uncertainty in the dose provided and vertical error bars indicating the variation between the cards. The graph shows that the response based on the Cs-137 cards have a higher sensitivity (steeper slope) and a higher correlation (R^2) than those irradiated with Co-60; this suggests that the cards may respond with higher predictability (using a dose-response function) and sensitivity at lower energy gammas.

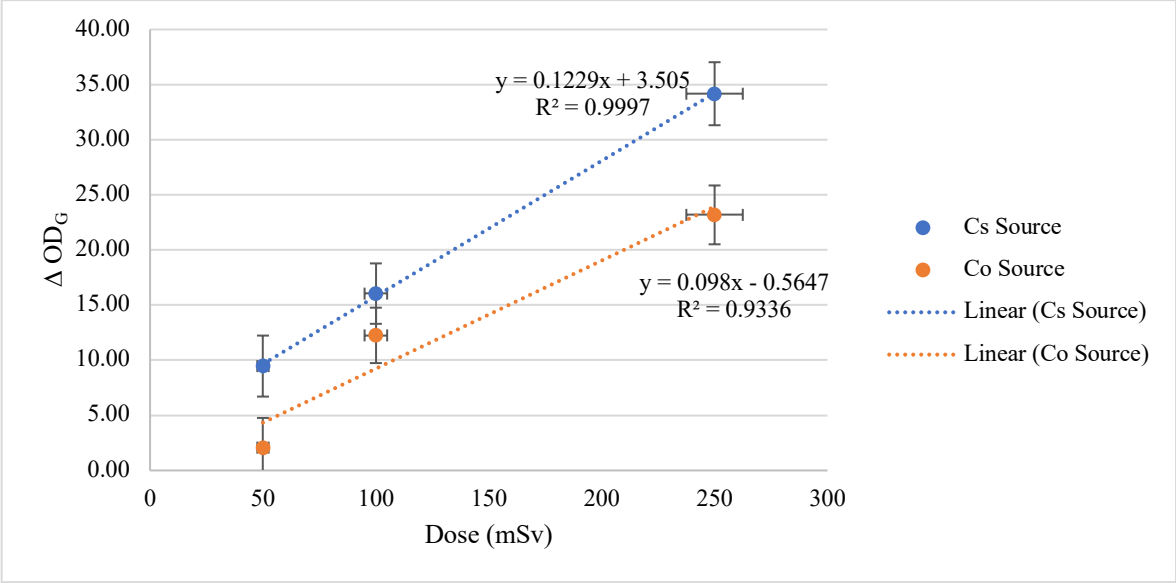

Figure 6.6: RadTriage Response as a Function of Gamma Energy. The plot shows the observed RadTriage responses; one set of results was acquired using a Cs-137 source and one set of results was acquired using a Co-60 source. The two sets can be compared to view the variation of the responses as a function of gamma energy.

The results for the TLD chips, also tested using two different gamma energies, is shown in Figure 6.7. The results here show that there is not a significant difference for TLD response as a function of gamma energy, but that if there is it may increase as a function of dose. Once again, vertical error bars indicate propagated uncertainty in TLD response and horizontal error bars indicate uncertainty in dose provided, based on the ionization calibration.

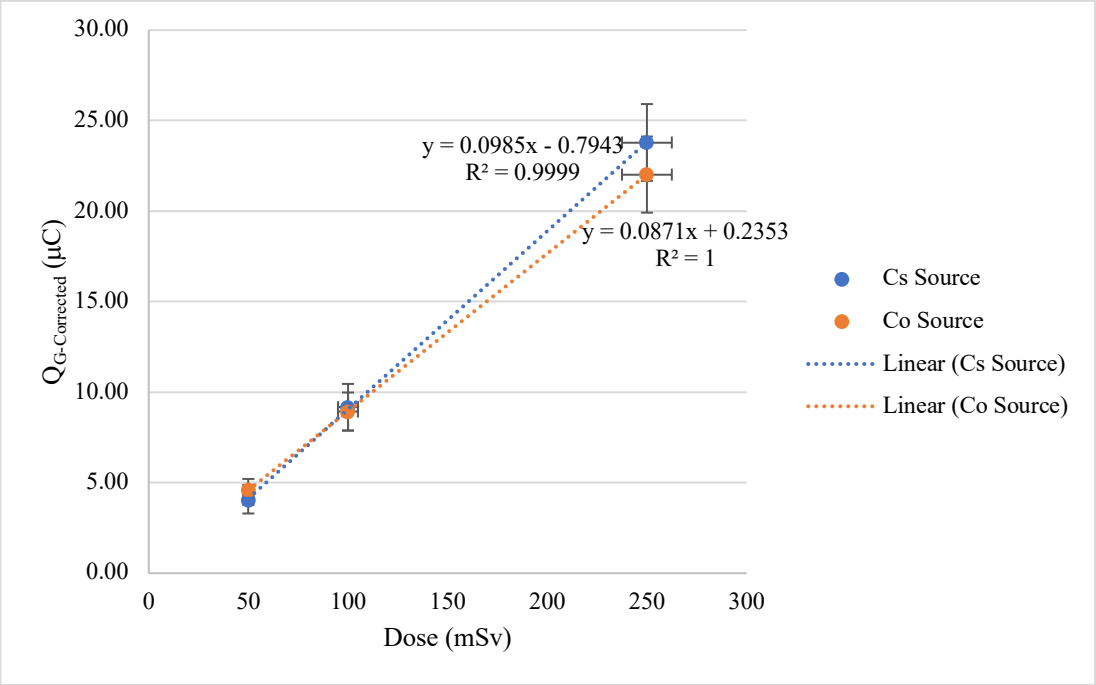

Figure 6.7: TLD Response as a Function of Gamma Energy. The plot shows the observed TLD responses; one set of results was acquired using a Cs-137 source and one set of results was acquired using a Co-60 source. The two sets can be compared to view the variation of the responses as a function of gamma energy.

CHAPTER 7: DISCUSSION

General Summary

The results for tests across the dose range, shown in Figures 6.1 and 6.2, indicate that the RadTriage cards, analyzed using P(D), respond with appreciable differences within the range specified by the manufacturer and that densitometry with a common scanner is able to map and quantify these response differences. At lower doses, the cards respond in a linear function, at higher doses the function levels off, making the overall dose response function exponential. This expands upon the work reviewed in the background section by providing a specific, quantified dose-response function. [15, 21]

Furthermore, testing at the low dose range, below that specified by the manufacturer, shows that the use of a scanner for densitometry analysis extends the operable range below the 50 mSv minimum. This research was able to extend the dose range by 40 mSv, to 10 mSv. The results, shown in Figure 6.3, were able to show how the group response at low doses was linear, however, the uncertainty for any specific card has a considerably wide range which could make it difficult to pinpoint an exact dose with just one sample. This also suggests uncertainty may have been overestimated.

The RadTriage card response as a function of dose rate and gamma energy was also investigated, shown in Figures 6.5 and 6.6. The plots suggest that there is a difference between the dose responses depending on the dose rate and gamma energy of the exposure. However, plotting alone cannot prove that there is a statistically significant difference between two means, which can often be misleading. For this reason, a T-test for two samples with two different means was used to determine if there is a statistical significance in the difference between the means for each of the two tests (dose rate and gamma energy). The equation for the Student T-Test is given by:

$$\textbf{Equation 7.1} \quad t = \frac{\overline{X_1} - \overline{X_2}}{\sqrt{\frac{S_1^2}{N_1} + \frac{S_2^2}{N_2}}},$$

where $\overline{X_1}$ is the mean of a group, in this research referenced as ΔOD_G, S_1 is the standard deviation of that group, and N_1 is the number of samples in that group. The results for the two Student T-Tests performed are shown in Tables 7.1 and 7.2 below; statistically significant differences, defined as surpassing a 95% certainty threshold (a generally accepted significance level of 0.05), are marked with an asterisk.

Table 7.1: Statistical T-Test for RadTriage and Gamma Energies

Dose (mSv):	50	100	250
CS Mean	129.69	123.11	104.98
Co Mean	137.08	126.82	115.97
CS N	7	7	7
Co N	10	10	10
Cs St Dev	2.77	2.74	2.86
Co St Dev	2.69	1.29	2.67
T value	**5.48***	**3.33***	**8.01***
(Threshold for 95% certainty = 1.96)			

This table displays the results for statistical T-Tests conducted to determine if the RadTriage mean response resulted in statistically significant variance based on different gamma energies. Statistically significant results are marked with an asterisk (>1.96).

Table 7.2: Statistical T-Test for RadTriage and Dose Rates

Rate (mSv/hr)	Response	StDev	T Value (vs 667)	T Value (vs 298)	T Value (vs 107)
667	123.11	2.74	**X**	**-1.26**	**-2.93***
298	121.38	2.85	**1.26**	**X**	**-1.68**
107	119.49	2.13	**2.93***	**1.68**	**X**

This table displays the results for a series of statistical T-Tests conducted to determine if the RadTriage mean response experienced statistically significant variance based on different dose rates. Statistically significant results are marked with an asterisk (>1.96).

The tests show that there are instances of statistically significant differences for both dose rate and gamma energy variances, where 1.96 is a T-Test score large enough to indicate statistical significance at 0.05 significance level (a 95% certainty level).

The RadTriage card response as a function of dose rate appears to be on the edge of statistical significance, and ought to be tested further in future work, and at broader ranges of dose rates. However, this research found a statistically significant difference for dose rate in the response of the RadTriage cards. The results also technically show a lower standard deviation at lower dose rates, but this is very likely impacted by the geometry of the radiation range and the minimization of any specific card and the source, and most likely not impacted by the rate itself. However, the possibility that dose rate also impacts response uniformity cannot be ruled out.

Finally, the results show that the card response has a very high likelihood of being affected by gamma energy and is more responsive, meaning increased sensitivity and greater ΔOD_G, at lower energies. This is supported by the fact that the different gamma energies produced statistically different responses for all three of the doses tested (Table 7.1). Once again, this was predicted by previous research. The variation for these specific responses were fairly small on the order of magnitude compared to the response itself, suggesting stronger results than those for the low dose tests.

Comparison to TLD Response

In general, the TLDs were able to produce a dose response function approximation with a better fit (higher R^2 value) than the RadTriage cards both at the specified dose range for the RadTriage cards and at low doses, shown in Figures 6.2 and 6.4. However, it is worth pointing out that the chips selected were those that responded relatively similarly (explained in Appendix B), so this could have played a role in the

TLD chips outperforming the RadTriage cards with respect to regression fitting and minimizing standard deviation. However, with respect to dose rate and gamma energy, the TLD chips certainly outperformed the RadTriage cards, in that they did appear to respond differently when these exposure characteristics changed, shown in Figures 6.5 and 6.7. To be consistent with the RadTriage card analysis, these differences across dose rate and gamma energy were tested with a Student T-Test, shown in Tables 7.3 and 7.4. Assuming the same significance level used for the RadTriage cards, 0.05 or 95% certainty, the TLD chips had no instances of statistically significant mean variance based on a change in dose rate or gamma energy.

Table 7.3: Statistical T-Test for TLDs and Gamma Energies

Dose (mSv):	50	100	250
CS Mean	4.04	9.17	23.79
Co Mean	4.60	8.93	22.02
CS N	10	10	10
Co N	10	10	10
Cs St Dev	0.74	1.29	2.12
Co St Dev	0.60	1.05	2.10
T Value	**1.85**	**-0.45**	**-1.88**
(Threshold for 95% certainty = 1.96)			

This table displays the results for statistical T-Tests conducted to determine if there was a statistically significant variance (T> 1.96) between the mean TLD responses based on gamma energy.

Table 7.4: Statistical T-Test for TLDs and Dose Rates

Rate (mSv/hr)	Response	StDev	T Value (vs 667)	T Value (vs 298)	T Value (vs 107)
667	9.17	1.29	**X**	**-0.53**	**-0.76**
298	8.84	1.16	**0.53**	**X**	**-0.22**
107	8.74	0.90	**0.76**	**0.22**	**X**

This table displays the results for a series of statistical T-Tests conducted to determine if there was a statistically significant variance (T> 1.96) between the mean TLD responses based on dose rate.

Time Elapse Characteristics

Interestingly, it was noticed that the color on the card visibly fades within a day or two, but that once the card is scanned, even if the color is faded, the same initial change in OD will be noticed by the scanner. This suggests that there could be a considerable window within which to scan a card and still be able to measure exposure. Although this observation was not tested thoroughly in this research, due to not recognizing the response until well into the research, data was still recorded for the change in the card response over a period of 6 weeks. Table 7.5 shows that the $P(D)_G$ dependence on whether the card is scanned within a day of exposure versus six weeks is statistically significant. This is consistent with what the AAPM results suggested, that most OD change occurs within 24 hours, but that additional OD change can continue long after the irradiation as a result of delayed chemical reactions. [3]

Because the cards were all scanned at the same amount of time post-irradiation for each test, there is no concern for this affecting the results of this research. However, if the cards are to be dispatched by governmental agencies for emergency responders, and then read after an exposure, it could be important to know how long after the exposure the cards were read. Thus it would be necessary to have more data on what the impact of this delay in scanning time is on the dose response of the card.

Table 7.5: Statistical T-Test for RadTriage P(D) Before and After 6 Weeks

	P(D)	StDev	T-Test
Prompt	104.98	2.86	**2.028***
post 6 weeks	101.96	2.71	

This table shows the different P(D)s detected based on whether the batch of cards was scanned within a day of the irradiation (noted as prompt) or six weeks after the irradiation (post 6 weeks). The T-Test value result is also provided, where significant values (T>1.96) are marked with an asterisk.

Batch Uniformity

It was also found throughout the research that the batch uniformity for the RadTriage cards was consistent. The cards had a fairly constant standard deviation measured within each group, and no major outlier cards were found throughout testing. Additionally, uniformity within the cards themselves, based on the standard deviation of the sensor strips ROI P(D), was consistent; the cards all had roughly the same standard deviation when their pixel density was measured in ImageJ, suggesting that the density of the polymers within the gels is fairly uniform and that there are not blotchy areas or cards with lower concentrations of polymers.

Comments on Testing Uncertainty

Although uncertainty was limited as much as possible, there are still factors of uncertainty that could not fully be accounted for. Although the tests were conducted on different days, the ionization chamber calibration, discussed in Appendix A, allowed for variations in humidity and temperature to be accounted for in the expected dose. However, other potential variants in dose could have arisen based on radial distance of certain TLD chips and cards from the direct gamma beam. This is because the TLD chips were located in the middle and the cards radially outward around the chips. This could have led to slight variation among the cards and could have increased the standard deviation slightly. However, this distance was, at a maximum 5 cm, and with the closest distance being 100 cm, this would be a relatively negligible distance. But it is still worth noting that this could have contributed to increased card standard deviation.

Another potential source of uncertainty would be the background accumulation of the cards throughout the period of testing. Testing took place over a period of 6 weeks and it is possible that certain cards at the end of the testing period could have been

affected by the accumulation of background dose throughout this time period. However, this background accumulation would have been extremely low compared to the minimum dose of 10 mSv that was tested in this research. Additionally, this was accounted for by taking blank card readings throughout the testing period; no significant change was noted over the period of time for testing. However, these tests were rudimentary, simply to verify no major changes; future research should put greater emphasis on monitoring potential background accumulation. Additionally, uncertainty based on whether or not scanning altered the response of the card was tested by scanning a card for a large number of times. No change was found based on multiple scans of the card. The data for this test can be found in Appendix D.

Finally, with respect to the TLDs, it should also be noted that previous research has found TLDs to have decay responses as a function of the number of times the chip was annealed. Thus, it is possible that there would have been a decay over the testing period in the responsiveness of the chips. There would be no way to account for this though, other than testing with new chips each time, and in that case new population and chip ECFs would have to be calculated for each test. [37]

CHAPTER 8: CONCLUSIONS

Summary of Findings

This research has found that RadTriage cards are able to be read with a commercial scanner using densitometry analysis to create a calibration curve with a high probability of fit ($P>0.99$). The RadTriage cards are able to indicate a change in optical density below the manufacturer-specified response range minimum of 50 mSv when using a commercial scanner and densitometry analysis. At low doses the cards have a linear response to radiation. At higher doses the cards have an exponential response to radiation. Together, these characteristics mean that the comprehensive response function to dose should take the exponential form.

This research also investigated exposure characteristics that could affect the sensitivity of the RadTriage cards, and thus create uncertainty in the dose response. The research results show, through partially statistically significant results, that the irradiation dose rate may have an impact on the responsiveness of the RadTriage cards. The results also show, through statistically significant results, that gamma energy impacts the responsiveness of the RadTriage cards. The RadTriage cards were found to respond more sensitively, resulting in a greater change in optical density, to Cs-137 gamma energy than to Co-60. The implication for these findings is that exposure characteristics would likely impact the response of the cards, and thus without a set of correction factors and knowledge about the exposure characteristics would increase the uncertainty in the dose found using scanning densitometry on the colorimetric response of the RadTriage cards.

Recommendation to Governmental Agencies with First Responders

The results of this research indicate that RadTriage cards could be a good tool to provide for routine use by emergency first responders. RadTriage cards are able to

immediately indicate dose to personnel that may have minimal knowledge of radiation detection and dosimetry. At the same time, this research has shown that they could be used post hoc with a common, flatbed scanner and a publicly-available image processing software to get a reasonable dose estimate. Problems may arise in determining a specific dose based on the gamma energy of the exposure source and on the dose rate of the exposure, among other exposure characteristics. But, on the whole, some dose estimate could be provided. Despite uncertainties that this research has shown would be inherent in the determined dose, a dose estimation within a certain range of accuracy is still better than the alternative of no dose estimation.

Based on these results, governmental agencies and other first-responder coordination organizations should consider investing in RadTriage cards, especially when faced with cost limitations that would otherwise prevent dosimeter dispatching. RadTriage cards would be especially useful when used in coordination with TLD chips, but even alone (assuming the alternative is no dosimeter at all) could provide their own unique benefits in the form of immediate indication of dose and ease of use. Furthermore, the RadTriage cards, which only require a standard commercial scanner to be read, may allow for a significantly cheaper bulk dispatch of dosimeters when compared to TLDs, which must be read with special TLD reading equipment, and by trained personnel.

However, if they are dispatched, RadTriage cards should only be used as real-time binary indicators of whether or not a dose is imminent while in the field. This is because the comparison to the reference images does not allow for a standardized dose reading, especially when considering the limits of the human eye in distinguishing between multiple shades of gray. Despite this limitation for real-time dose determination, carrying

the RadTriage card would still allow for subsequent quantification of the dose using the scanning densitometry methodology once out of the field.

Broader Applicability

Beyond utility for first responders, RadTriage cards may be useful to members of the general public who are concerned about possible radiation exposure. The cards could be placed around the house in case of an emergency; after an emergency, or an expected exposure, the person in possession of the RadTriage cards could measure dose relatively easily without any special equipment. While this would result in a positive outcome if it means that citizens begin to grow more invested in understanding their radiation dose, it could also create a problem if citizens mishandle their cards and become alarmed over a resulting false positive.

CHAPTER 9: RECOMMENDATIONS FOR FUTURE RESEARCH

Further efforts to conduct research on RadTriage cards should emphasize techniques that could be used to read cards after events with greater certainty. Improving the accuracy of the dose response function would allow for increased utility of the cards.

The first step to achieving a usable dose response function with increased certainty would be maximizing the statistical power of the function. This research was limited in the amount of power it was able to achieve due to limits on the cards provided and the laboratory time allocated. However, if such a function is deemed to be desired, one with greater power could be found through larger sample sizes. Additionally, increasing certainty in the baseline function could be achieved through creating a more comprehensive calibration curve, and filling in more doses throughout the range of use. Finally, expansion of the baseline function could include breaking down the function into the linear and exponential components and determining if using only one of these functions at specific dose ranges is more beneficial than using the complete dose-response function.

This research has also proven that using such a function for dose approximation would require the establishment of correction factors to the function based on certain exposure characteristics. Research to establish such correction factors would require quantitatively measuring the effect of gamma energies and dose rates, and specifically the impact of these characteristics across the dose range of the card. Other exposure characteristics not studied in this research should also be considered, including the possibility of incidence angle of the exposure and material encasing or surrounding the RadTriage card (such as if the card is worn on a person or placed on a wall).

Furthermore, this research was conducted with one manufacturing batch of cards. If quantification of the RadTriage response using a dose response function were to become a more established practice, there would have to be tests of inter-batch homogeneity to ensure that each batch has the same properties. Otherwise, if batches do end up varying slightly, then perhaps one card of each batch could be used to create a coefficient to standardize all of the cards in that batch. This may also be important in establishing a correction factor for the age of the batch, as older batches may have accumulated more background radiation than newer batches.

Finally, other scanning and densitometry methods could be tested to determine the ideal conditions for other scanning methods that would be sufficient for a dose estimation. For instance, it may be useful to know if the use of smart phone cameras could be substituted for commercial scanners to perform the densitometry analysis. Many smart phones can download software to use the built-in camera as a scanner. This may be useful in the case where emergency response workers or civilians do not have access to a scanner. It may also be useful if such a software can be created that would include densitometry analysis and the dose response function to automatically calculate the dose estimate, all in one. This type of application would provide many benefits, especially if it prompts the user to fill out characteristics about the exposure to the best of their knowledge, and then incorporates the knowledge into performing a dose calculation. This could effectively eliminate user error from the process of dose reconstruction.

APPENDIX A: IONIZATION CHAMBER CALIBRATION

As stated in the materials and methods text, a spherical ionization chamber was used to achieve a calibrated dose for each test. This allowed for a precise dose rate determination that could then be used to determine the amount of time required for each test to achieve a specific dose. Ionization chambers are common methods for acquiring precise exposure determinations.

Using an ionization chamber requires the application of a high bias voltage to the central and outer electrodes, shown in Figure A.1, at the inner tube and outer spherical shell, respectively. When exposure is incident, the radiation interacts with the gas filling the chamber, which ionizes the electrons of the gas and creates a current. Thus, the measure of the change in current charge, dQ, per the volume of the chamber, dm^3, can give a proximate exposure determination: $X = dQ/dV\ (m^{3)}$.

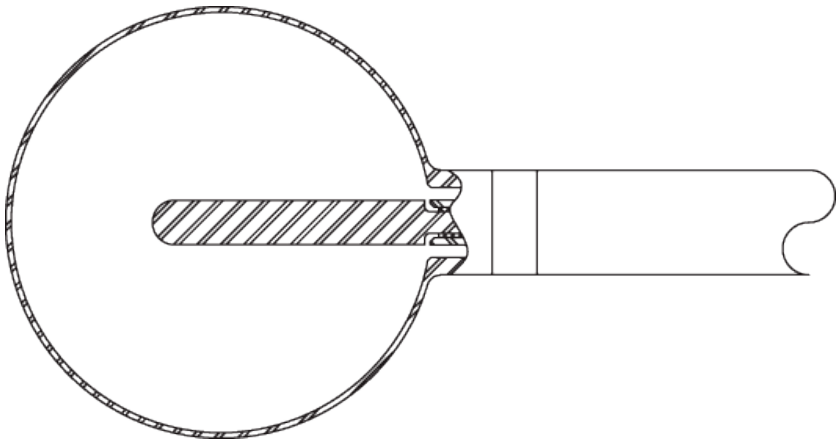

Figure A.1: Ionization Chamber Diagram. A spherical ionization chamber like the one used for this research is shown. This image is publicly available from Exradian (Middleton, WI).

In calibrating the dose rate for this research, the ionization chamber was irradiated for three one-minute trials. Figure A.2 shows the spreadsheet that was used to calculate an average dose rate and standard deviation using the result from the trials. The spreadsheet also incorporates corrections for ambient temperature and pressure differences.

Performing this procedure for each test ultimately allowed for the minimization of uncertainty from potential changes in dose rate based on temperature, pressure, and humidity factors.

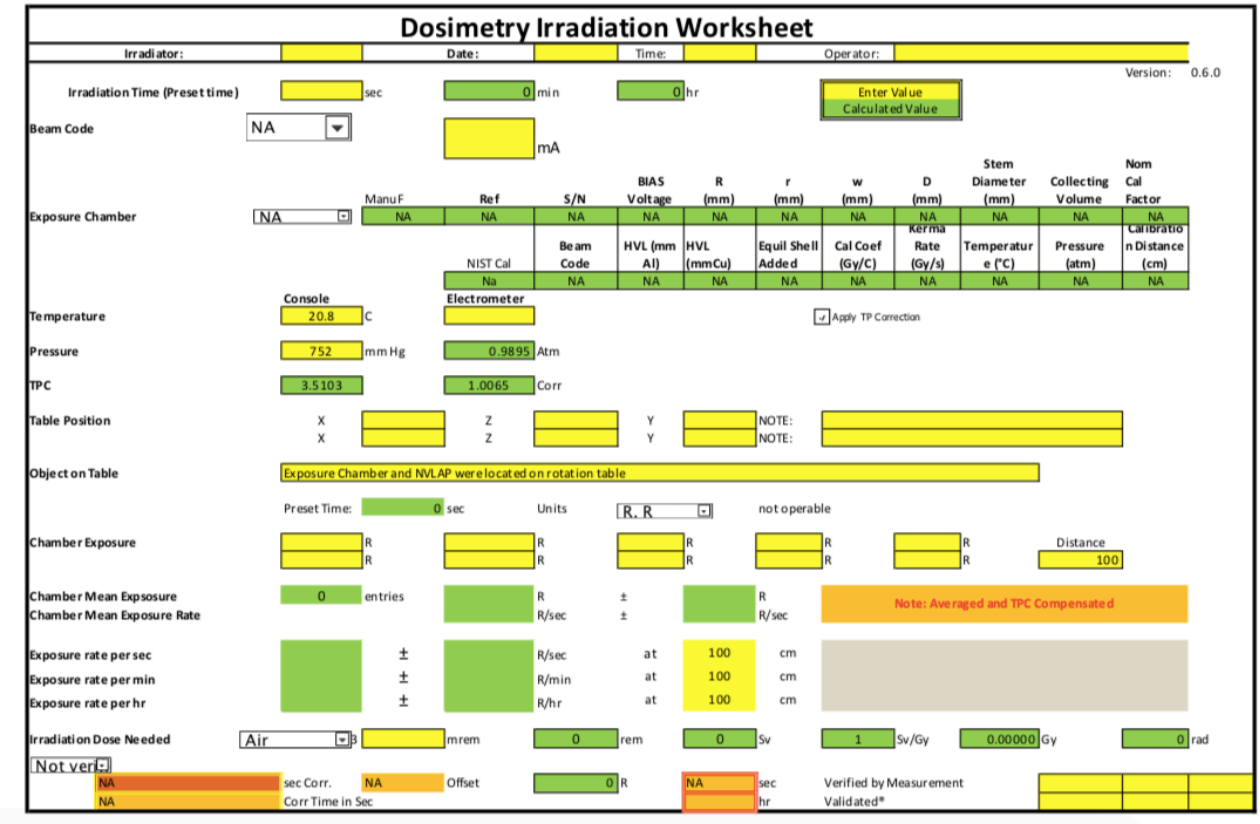

Figure A.2: Ionization Chamber Calculation Worksheet. This worksheet contains the calculations used to correct the ion chamber results for temperature and pressure across trials. This spreadsheet was created by Dr. Luis Benevides at NSWCCD (Bethesda, MD).

APPENDIX B: TLD ECF DETERMINATION

This section will discuss the procedure used to get a population average for the LiF:MCP chips and discuss how the chips were selected from a larger sample.

Materials

This procedure used 86 LiF:MCP TLD chips and a Harshaw (Waltham, MA) QS 3500 TLD reader supplied with nitrogen gas. The HarshawQS TLD reader was operated using a personal computer that had WinREMS (Waltham, MA) interface software downloaded onto it.

The same reading settings on WinREMS and procedures were used for all annealing and reading of the TLD chips. The settings designated a calibration region of 1-200, a preheat temperature of 165 °C in 10 seconds, an acquisition temperature rate of 15 °C/second with a maximum temperature of 260 °C (below the 270°C threshold for damaging the chips, as mentioned in the background section), with a total acquisition time of 16.667 seconds. These setting properties are referred to as the Time Temperature Profile (TTP). Throughout the annealing process, this TTP acquisition cycle was repeated until the chips reached a threshold of around 1.5 nC or less.

For irradiation, a Hopewell Designs LLC (Alpharetta, GA) Model GC-60 Bamma Beam Irradiator (GC60), along with a Cs-137 source were used to deliver known radiation doses to TLD chips. During irradiation, the TLD chips were placed on an acrylic phantom fit with 100 individual wells.

Annealing

The TLD chips were initially annealed before the first irradiation because they had been stored, unused in the lab for around 12 months, thus they had accumulated a non-negligible background dose. The annealing readings were recorded incase needed for

future use. The chips were annealed until they met a threshold of around 1.5 nanocoulombs, which took about two to three reads per chip.

Initial Calibration

Calibration was performed to obtain a reader calibration factor (RCF) as outlined by Moscovitch *et. al*.. This required the TLDs to be annealed, and then irradiated with a known dose, L. Then, the TLDs were read and an average measured charge, <Q> was determined. All of the chips except for four were placed in individual wells in the phantom to be irradiated. The four remaining chips were used as controls to acquire the background dose over the course of the testing. The known dose, L, was provided to the chips in the phantom with the Cs-137 source at a distance of 300 cm with a dose rate of 6048 mR/hr or a time of 200 seconds, resulting in a total dose of 336 mR. After the chips were irradiated, they then were read using the same procedure specified in the materials section.

While reading the chips, it became obvious that a few of the chips were composed of a material other than LiF:MCP. They appeared visibly darker and did not have glow curve peaks in the region of interest. There were also chips that were square in shape and that also provided response values very different from the LiF:MCP chips (by an order of magnitude). The data from these chips was recorded but was not included in the sample population data calculations.

Results

Upon reading all of the chips from this irradiation, it became apparent that there were two separate sets of chips, even without accounting for the chips previously mentioned that were noticeably different materials. Although it was believed that all of the LiF:MCP chips should be treated the same, there were two distinct groups of chips

noticed. This suggests that the chip sets were either produced in different batches, and thus had different dopant levels, or that the chips had been irradiated a different number of times (having lost sensitivity).

Each of the chip sets (one which had been labeled by the previous user in a numeric system of 1-100, and the other which had been labeled by a previous user in a triple digit system) were analyzed separately to produce a population mean and standard deviation. One set (here out called Set 1) had a mean of $\langle Q_1 \rangle$= 347 nanocoulombs and the other set (here out called Set 2) had a mean of $\langle Q_2 \rangle$= 439 nanocoulombs. They each had large standard deviations as well: σ_1= 46nC and σ_2= 63 nanocoulombs, with sample sizes n_1 = 36 and n_2 = 43.

A difference of means student T-Test was used to determine if the populations were significantly different. Using the equation,

$$t = \frac{\overline{X_1} - \overline{X_2}}{\sqrt{\frac{\sigma_1}{n_1} - \frac{\sigma_2}{n_2}}},$$

a T value of 7.49 was determined. This is compared to a required value of 1.96 in order to prove with 95% certainty that the sets are different, thus the T value greatly exceeded the required value, confirming the conclusion that the two sets are different.

Additionally, the individual RCF values were calculated. Again, this is simply the ratio: RCF = $\langle Q \rangle$/L, where L is the dose the chips were exposed to. By finding the mean of each of the sets of TLD chips, the average group RCFs were found, RCF_{G1} = 1.03 nanocoulombs/mR and RCF_{G2} = 1.31 nanocoulombs/mR, and the total population was found to be RCF_T = 1.17 nanocoulombs/mR. This can thus be used in later trials to predict a relative amount of dose for an unknown exposure based on the TLD reading acquired, assuming it is known which population the chips are from. However, it can be seen that the calibration factors are significantly different depending on the population,

and thus if the sample the chip is pulled from is not known, the estimated dose could vary significantly.

Selecting a Sample Population

For the purpose of finding a set of TLD chips to be used in comparison to RadTriage cards, each chip was given its own element correction factor, ECF, or a ratio that would standardize each chip response to the population mean. A group of 30 chips were chosen from the population based on their ECFs and specifically, the proximity of the ECF to 1.0 (which would mean the chip is closest to the population average).

The chosen chips were then placed into one of three groups, with each group consisting of 10 chips. The purpose of placing the chips into groups was so that there would be three sets to use for testing. The resulting chips and groups selected are provided in Table B.1, along with the chip ECF to standardize the chip response to both the population and to the group it was placed in. Each group was given a group ECF as well. The purpose of the group ECF was to standardize the group average response to the 30-TLD population response. This means, that regardless of which group is used for any given test, the resulting group average could be corrected to ensure that a small difference between groups would not occur. This is essentially the same result as using individual ECFs for each of the chips, but since the specific chips in each group didn't change throughout testing, a group ECF allowed for quicker analysis, while achieving the same resulting corrected TLD mean response.

Table B.1: TLD Chips Chosen for Testing and ECF Values				
New Number	Old Number	Q (nanocoulombs)	ECF to Group	ECF to Population
1	741	486.25	0.89	0.87
2	141	501.30	0.92	0.89
3	361	579.96	1.07	1.03
4	551	517.49	0.95	0.92
5	751	524.85	0.97	0.94
6	841	601.95	1.11	1.07
7	341	437.84	0.81	0.78
8	921	680.45	1.25	1.21
9	861	584.54	1.08	1.04
10	441	518.81	0.95	0.93
Avg		543.34		
1-10 Group ECF		**0.97**		
11	941	555.35	0.99	0.99
12	121	590.17	1.05	1.05
13	771	519.91	0.93	0.93
14	821	702.04	1.25	1.25
15	451	528.09	0.94	0.94
16	261	524.39	0.93	0.94
17	461	553.76	0.99	0.99
18	951	601.30	1.07	1.07
19	661	526.33	0.94	0.94
20	241	512.08	0.91	0.91
Avg		561.34		
11-20 Group ECF		**1.00**		
21	931	489.90	0.85	0.87
22	851	636.99	1.10	1.14
23	1021	630.11	1.09	1.12
24	541	521.90	0.90	0.93
25	961	604.80	1.05	1.08
26	161	488.68	0.85	0.87
27	231	576.33	1.00	1.03
28	621	672.67	1.17	1.20
29	521	672.60	1.17	1.20
30	151	476.88	0.83	0.85
Avg		577.09		
21-30 Group ECF		**1.03**		
Total AVG		560.59		

In the table, ECFs were calculated through individual ECF and population average determinations. The group ECF was used to standardize each TLD group average in the research tested.

APPENDIX C: ROUTINE EQUIPMENT BACKGROUND VERIFICATION

Because the tests were conducted over a period of weeks, the equipment used to read the cards and TLDs after each test had to be continually tested, to ensure that it was not degrading over time and that there was no significant reading difference between trials. This verification was performed using the reference light and photomultiplier (PMT) background noise checks on the Harshaw QS Model 3500 (ThermoScientific, Waltham, MA), and by reading blank areas on the scanner.

For the reference light and PMT noise checks, readings were recorded after every ten times the instrument was run to check for variations in the dark current (PMT noise check) and for variations with a light of known emission (reference light check) to ensure there was no degradation in the instrumentation. For the scanner, the background light was checked for every single scan to ensure there was not variation in the lamp lumosity after a number of consecutive scans in addition to over time. The results are provided in Figures C.1, C.2, and C.3 below. Lines are drawn to indicate the upper and lower bounds using one and two standard deviations around the sample mean. For all checks, there is no significant noise beyond two standard deviations.

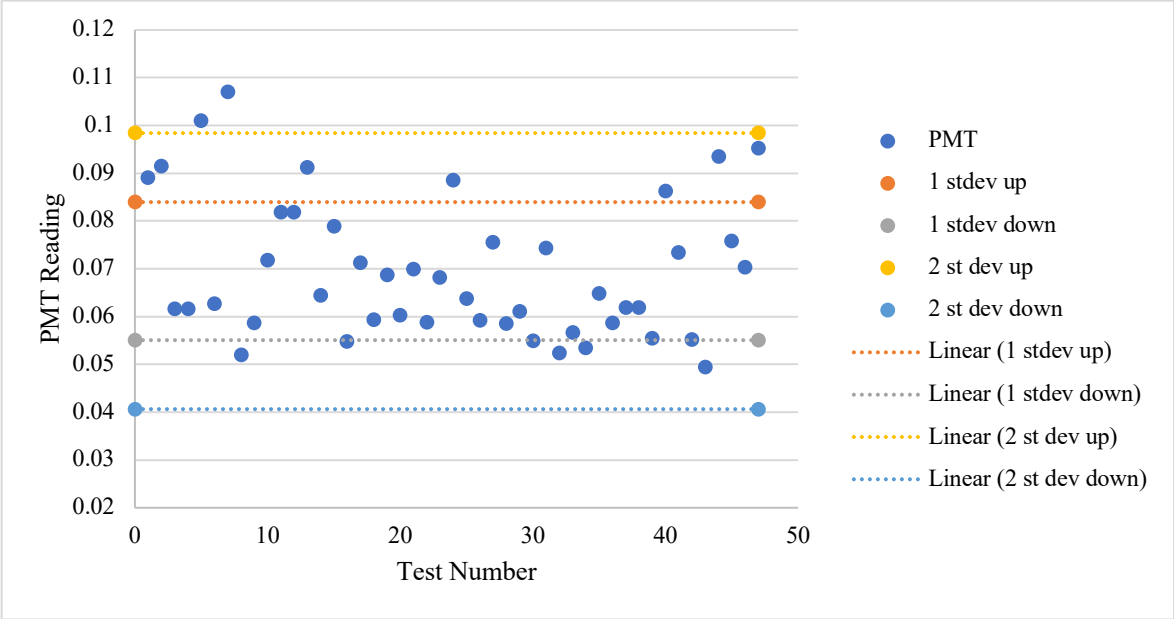

Figure C.1: PMT Noise Test. The results shown from the background PMT noise tests were used to verify that the readings from the Harshaw QS 3500 were accurate. Upper and lower bounds are shown at plus and minus one and two standard deviations.

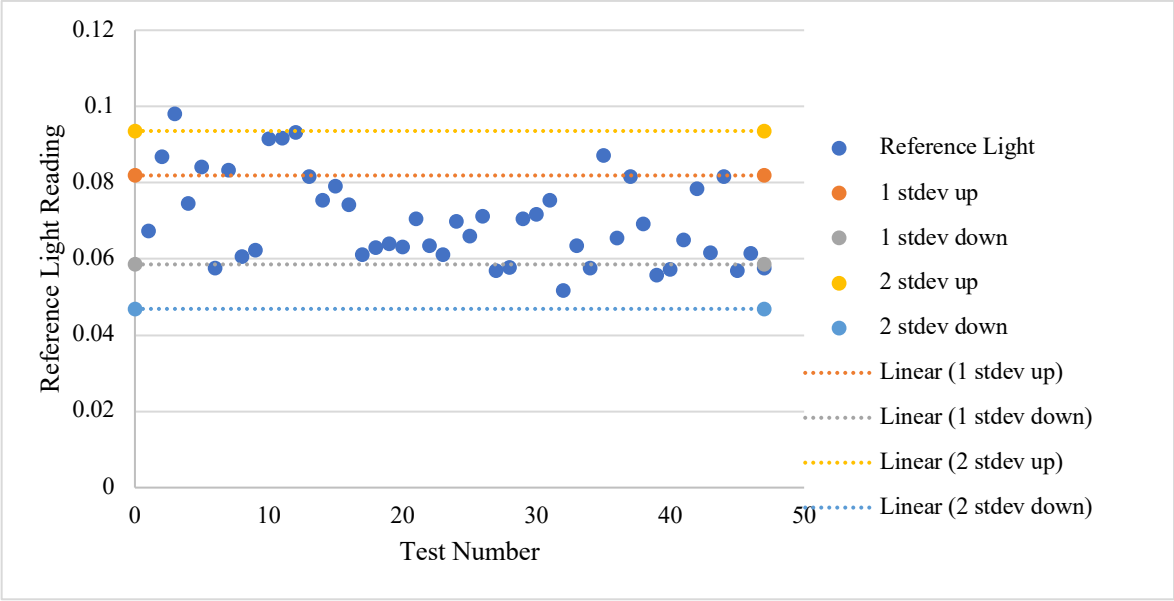

Figure C.2: Reference Light Background Test. The results shown from the background reference light tests were used to verify that the readings from the Harshaw QS 3500 were accurate. Upper and lower bounds are shown at plus and minus one and two standard deviations.

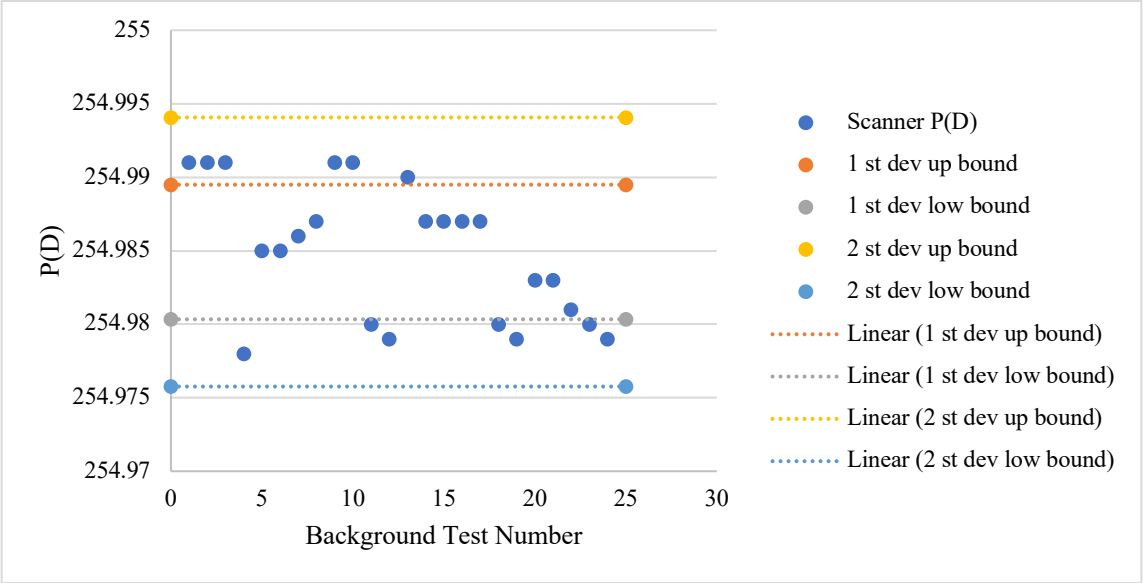

Figure C.3: Scanner Lumosity Test. The results shown from the scanner lumosity test were used to verify that the scanner light and quality were not deteriorating over time. Upper and lower bounds are shown at plus and minus one and two standard deviations.

APPENDIX D: CARD DETERIORATION OVER SCANS

The RadTriage cards were scanned 35 times, well beyond what would be necessary in real testing, to determine if the scanner light alone may affect the P(D) reading. The resulting data, presented in Figure D.1, shows that there is no clear change in P(D) as a result of numerous scans. Upper and lower bounds are indicated at one and two standard deviations above and below the population mean. Only two scans exceed upper and lower bounds.

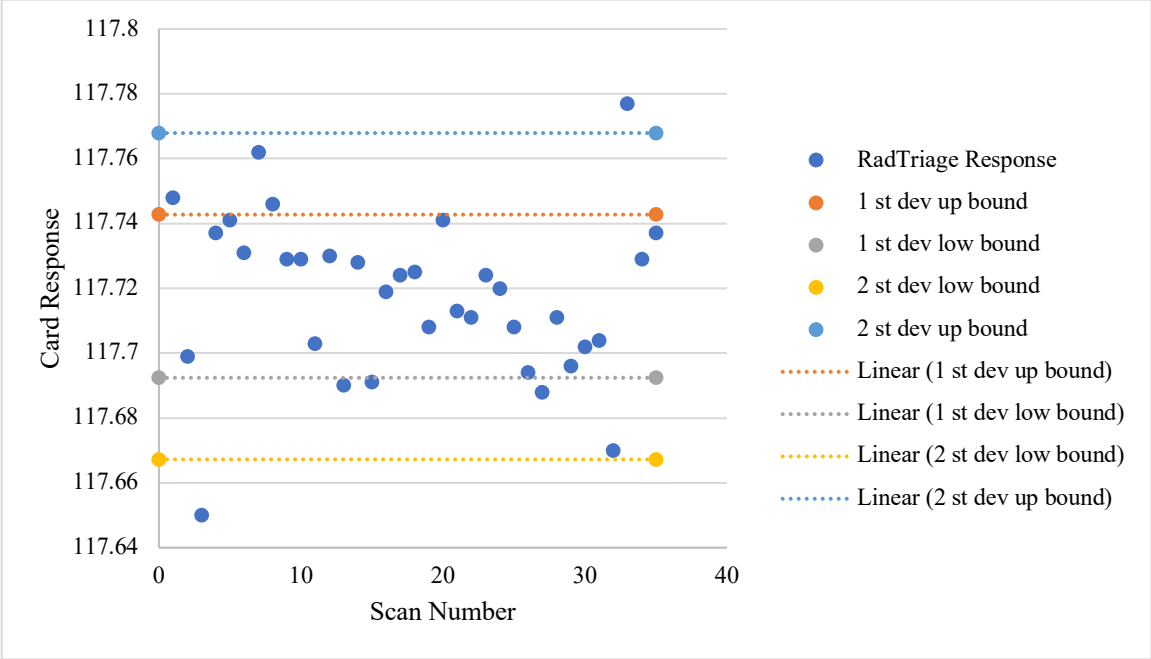

Figure D.1: RadTriage Response Over Repeated Scans. The results shown are the P(D) for a RadTriage card after 35 consecutive scans. There is no noticeable change in P(D) based on the number of scans. Upper and lower bounds are shown at plus and minus one and two standard deviations.

APPENDIX E: RESIDUAL TESTING FOR FIT DETERMINATION

Residual testing was used to evaluate the different fits tested for the RadTriage dose response curve. Initially a polynomial/quadratic function was used to fit the dose response curve, however the polynomial function did not allow for the plateau beyond the tested range that is known to occur due to the chemical characteristics (depletion of polymers) of colorimetric dosimeters. Thus, an exponential function was tested as it was able to satisfy the boundary conditions by allowing for a plateau at higher doses. The residuals were also minimized and slightly more randomized when using the exponential fit. The residuals for both fits considered are shown in Figure E.1 below.

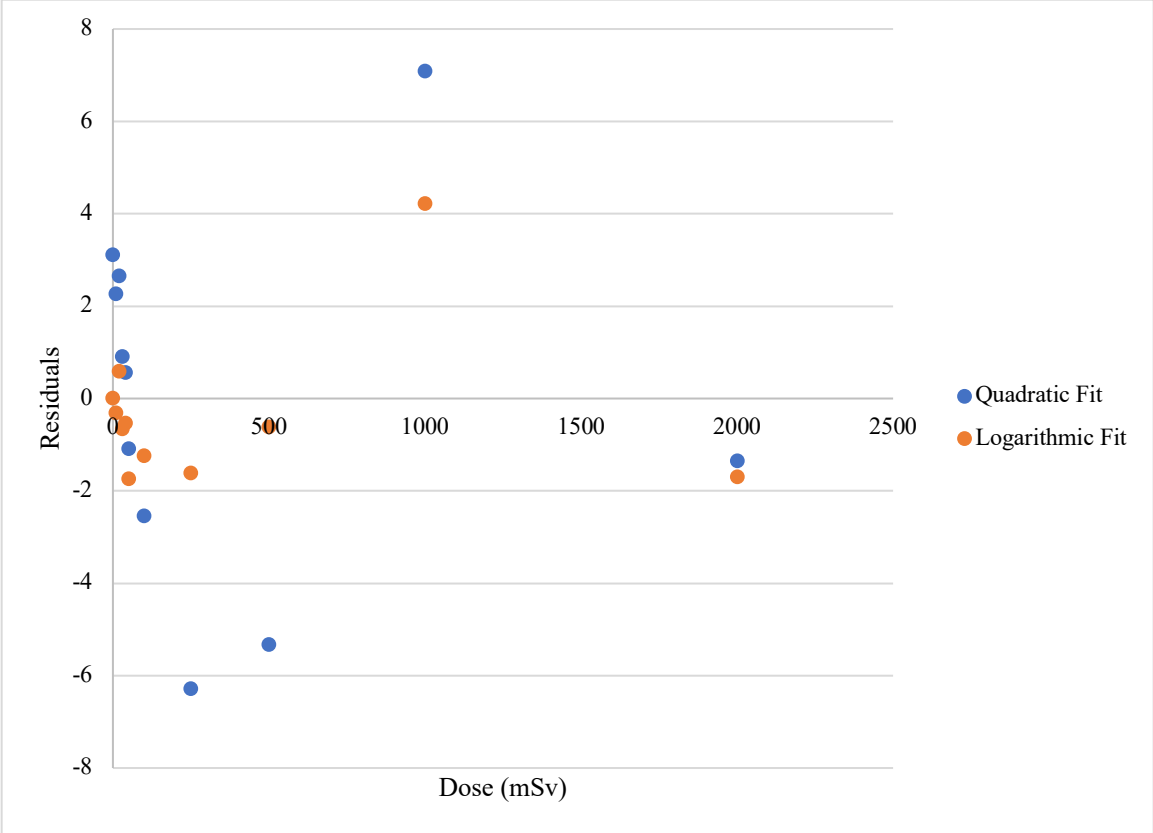

Figure E.1: Residuals for Fit Testing Plotted as a Function of Dose. The residuals for quadratic and the exponential fits of RadTriage data are shown. The residuals show the difference between experimentally observed data and the response predicted by the function used.

BIBLIOGRAPHY

[1] Klemic, Gladys, Bailey, Paul, Monetti, Matthew, Breheny, Cecilia, Hall, Howard, and Buddemeier, Brook. "Self-Indicating Instant Radiation Alert Dosimeter (SIRAD) Test Results Final Report." *Department of Homeland Security's (DHS) Science and Technology (S&T) Directorate's CounterMeasures Test Beds.* 2007.

[2] Jordan, Kevin. "Review of recent advances in radiochromic materials for 3D dosimetry." *Journal of Physics: Conference Series*. Pp. 250. 2010.

[3] Niroomand-Rad, Azam, Blackwell, Charles, Coursey, Bert, Gall, Kenneth, Galvin, James, McLaughlin, William, Meigooni, Ali, Nath, Ravindor, Rodgers, James, and Soares, Christopher. "Radiochromic Film Dosimetry: Recommendations of AAPM Radiation Therapy Committee Task Group 55." *American Association of Physicists in Medicine* vol. 25:11. 1998.

[4] Stewart, H. "Assessing and Evaluating the Self-indicating Instant Radiation Alert Dosimeter (SIRAD) for Gamma and Neutron Response." Oregon State University-Thesis. 2005.

[5] Patel, Gordhan, Patel, Jessica, and Patel, Pareshkumar. "Stick-on Self-Indicating Instant Radiation Dosimeter." United States Patent Office. 2007.

[6] Riel, Gordon, Winters, Patrick, Patel, Gordhan, and Patel, Paresh. "Self-indicating radiation alert dosimeter (SIRAD)." *Radiation Protection Dosimetry.* 2006.

[7] Riel, Gordon, and Rogalski, Rob. "Low Cost Self Indicating Casualty Dosimeter." Proceedings of the 21st International Dosimetry Symposium. Virginia Beach, VA, 2002.

[8] "Assessment of SIRAD neutron sensitivity." Oregon State University: A report to Technical Support Working Group and Gordhan Patel. 2006.

[9] American National Standards Institute/Health Physics Society Standard N13.11-2009, American National Standard for Dosimetry – Personnel Dosimetry Performance – Criteria for Testing, published by Health Physics Society, McLean VA.

[10] Le Guen, Bernard, Stricker, Laurent, and Schlumberger, Martin. "Distributing KI pills to minimize thyroid radiation exposure in case of a nuclear accident in France." *Nature Clinical Practice Endocrinology & Metabolism* vol. 3: 611. 2007.

[11] Soare, Christopher G., Trichter, Samuel, and Devic, Slobedan. "Radiochromic film." *Clinical Dosimetry Measurements in Radiotherapy*. 2009. Pp. 759-813.

[12] McLaughlin, W.L., C. Yun-Dong, C. G. Soars, A. Miller, G. Van Dyke, and D. F. Lewis. "Sensitometry of the response of a new radiochromic film dosimeter to

gamma radiation and electron beams." *Nuclear Instrumentation Methodology Physics Review* A302: 165-176. 1991.

[13] Oldham, Mark. "Radiochromic 3D Detectors." Journal of Physics: Conference Series 573 (2015).

[14] Devic, Slobodan. "Radiochromic film dosimetry: Past, present, and future." *Physica Medica* vol. 27. Pp. 122-134. 2010.

[15] Williams, Matthew and Metcalfe, Peter. "Radiochromic film dosimetry and its applications in radiotherapy." University of Wollongong, Australia: Faculty of Engineering-Papers. 2011.

[16] Yao, Tiantian, Leonard Luthjens, Alessia Gasparini, and John Warman. "A study of four radiochromic films currently used for (2D) radiation dosimetry." *Radiation Physics and Chemistry* 133:37-44. 2012.

[17] Ebert, Martin A., Asad, Ali H., Siddiqui, Salim A. "Suitability of radiochromic films for dosimetry of low energy X-rays." *Journal of Applied Clinical Medical Physics* vol. 10:4. 2009.

[18] Schreiner, L. J. "True 3D chemical dosimetry (gels, plastics): Development and clinical role." *Journal of Physics: Conference Series* 573. 2015.

[19] Amin, M. N., Horsfield, M. A., Bonnett, D. E., Dunn, M. J., Poulton, M., and Harding, P. F. "A comparison of polyacrylamide gels and radiochromic film for source measurements in intravascular brachytherapy." *The British Journal of Radiology* vol. 76: 824-831. 2003.

[20] Deene, Y. De., Hurley, C., Venning, A., Vergote, K., Mather, M., Healy, B. J., and Baldock, C. "A basic study of some normoxic polymer gel dosimeters." *Institute of Physics Publishing: Physics in Medicine and Biology* vol. 47. 2002.

[21] Chen, S. N., M. Gauthier, M. Bazalova-Carter, S. Bolanos, S. Glenzer, R. Riquer, G. Revet, P. Antici, A. Morabito, A. Propp, M. Starodubstev, and J. Fuchs. "Absolute dosimetric characterization of Gafchromic EBT3 and HDv2 films using commercial flat-bed scanners and evaluation of the scanner response function variability." *American Institution of Physics: Review of Scientific Instruments* vol. 87. 2016.

[22] Brodsky, Allen. "Personal Radiation Dose Monitors for the Public and Emergency Responders." *Journal of American Physicians and Surgeons* vol. 15:2. Summer 2010.

[23] Abdel-Fattah, Atef, and Miller, Arne. "Temperature, Humidity, and Time. Combined Effects on Radiochromic Film Dosimeters." *Radiation Physical Chemistry* vol. 46:4. 1996.

[24] Chelminski, Krzysztof, Bulski, Wojciech, Georg, Dietmar, Dominika Bodzak, Zbigniew Maniakowski, Dominika Oborska, Joanna Rostkowska, Malgorzata Kania. "Energy dependence of radiochromic dosimetry films for use in radiotherapy verification." *Reports for Practical Oncology and Radiotherapy* vol. 15. pp 40-46. 2010.

[25] Rink, Alexandra, Vitkin, I. Alex, and Jaffray, David A.. "Energy Dependence (75kVp to 18MV) of radiochromic films assessed using a real-time optical densitometer." *Medical Physics* vol. 34:2. February 2007.

[26] Abegaz, Sisay. "Beta Radiation Response of SIRAD Colorimetric Dosimeter vs Theoretical Calculation of Beta Dose in the 5 to 25 rad range." Georgetown University Graduate School of Arts and Sciences- Thesis. 2011.

[27] Cohen, S., A. Abraham, O. Pelled, Y. Tubul, E. Kresner, A. Ashkenazi, and I. Yaar. "Comparison Study of the Response of Several Passive PDA Based Personal Dosimeters to Gamma and X-Ray Radiation." *Dosimetry*. 2014.

[28] Bak, Alysse. "Assessing and Evaluating the Energy and Angular Dependence of Self-Indicating Instant Radiation Alert Dosimeters (SIRAD)." Oregon State University- Thesis. 2005.

[29] Kreit, Eric, Mathger, Lydia, Hanlon, Roger, Dennis, Patrick, Naik, Rajesh, Forsythe, Eric, and Heikenfeld, Jason. "Biological versus electronic adaptive coloration: how can one inform the other?" *Journal of the Royal Society* vol. 10: 78. 2013.

[30] Brady, Samuel, Yoshizumi, Terry, Toncheva, Greta, and Frush, Donald. "Implementation of radiochromic film dosimetry protocol for volumetric dose assessments to various organs during diagnostic CT procedures." *Medical Physics* vol. 37: 9. pp. 4782-4792.

[31] Knoll, Genn F. *Radiation Detection and Measurement* (Fourth Edition). John Wiley & Sons, Inc. pp. 751-758. 2010.

[32] Lee, J. I., Kim, J. L., Pradhan, A. S., Kim, B. H., Chung, K. S., and Choe, H. S.. "Role of dopants in LiF TLD materials." *Radiation Measurements* vol. 43. pp. 303-308. 2008.

[33] Moscovitch, M. "Personnel Dosimetry using LiF: Mg, Cu, P." *Radiation Protection and Dosimetry* vol. 85. pp. 49-56. 1999.

[34] Voss, S.P., Suchetta, A., Romanyukha, A., Moscovitch, M., Kennemur, L. K., and Benevides, L. A. "Effect of TLD-700H (LiF:Mg,Cu,P) sensitivity loss at multiple self-irradiation cycles on TLD reader calibration." *Radiation. Measurements* vol. 46**.** 1590-1594. 2011.

[35] Bilski, P., Budzanowski, M., Olko, P. "Dependence of LiF:Mg,Cu,P (MCP-N) Glow Curve Structure on Dopant Composition and Thermal Treatment." *Radiation Protection Dosimetry* 69. Pp. 187-198. 1997.

[36] Chen, Tai-Chang, Stoebe, Thomas. "Role of Impurities in the Thermoluminescence of LiF:Mg,Cu,P." *Radiation Protection Dosimetry. World Scientific Publishing Company.* 1998

[37] Romanyukha, Alexander, Delzer, Jeffrey, Grypp, Matthew, and Williams, Anthony. "Effect of Short-term sensitivity loss in LiF: Mg,Cu,P Thermoluminescence Dosimeter and its implications on personnel dosimetry operations." *Radiation Protection Dosimetry* vol. 168:2. pp. 204-211. 2016.

[38] Del Sol, F., Garcia-Salcedo, R., Mendoza, J., Sanchez-Guzman, D., Rodriguez, G., Goana, E., Montalvo, T. "Thermoluminescent Characteristics of LiF:Mg,Cu,P and $CaSO_4$ for low dose measurement." *Applications of Radioactive Isotopes* 71**.** Pp**.** 30-34. 2016.

[39] Moscovitch, M., Y.S. Horowitz. "Thermoluminescent materials for medical applications: LiF:Mg,Ti and LiF:Mg,Cu,P*." Radiation Measurements* vol. 41. 2007.

[40] Weinstein, M., Ben-Shachar, B., German, U., Levinson, S. and Lichtmann, I. "Environmental measurements employing different TLD's." International Atomic Energy Agency- Nuclear Research Center.

[41] Budzanowski, M., J.L. Kim, Y.M. Nam, S.Y. Chang, P. Bilski, and P. Olko. "Dosimetric Properties of sintered LiF:Mg,Cu,Na,Si TL detectors." *Radiation Measurements* vol. 33. 2001.

[42] International Atomic Energy Agency (IAEA)-European Radiation Dosimetry Group (EURADOS-7) Project, IAEA technical document 1564, Intercomparison of Personal Dose Equivalent Measurements by Active Personal Dosimeters. IAEA, Vienna. 2007.

[43] Johnson, Jr., Raymond. "Chapter 15: Radiation Instrument Training: Six Challenges for Emergency Responders." *Public Protection from Nuclear, Chemical, and Biological Terrorism*, Editors: Allen Brodsky, Raymond Johnson, Ronald Groans. Pp. 241- 292. 2004.

[44] Kouzes, Richard T. "Chapter 3: Radiation Detection and Interdiction for Public Protection from Terrorism." *Public Protection from Nuclear, Chemical, and Biological Terrorism*, Editors: Allen Brodsky, Raymond Johnson, Ronald Groans. 2004. Pp. 17-29.

[45] O'Connell, Tom, Ares, Paul. "Chapter 11: An Approach to First Responder Radiological Preparedness." *Public Protection from Nuclear, Chemical, and*

Biological Terrorism, Editors: Allen Brodsky, Raymond Johnson, Ronald Groans. Pp. 139-141. 2004.